Monthly Notices of the ROYAL ASTRONOMICAL SOCIETY

MNRAS **462,** 2950–2969 (2016) doi:10.1093/mnras/stw1841
Advance Access publication 2016 July 28

MOCCA-SURVEY database I. Accreting white dwarf binary systems in globular clusters – I. Cataclysmic variables – present-day population

Diogo Belloni,[1,2]★ Mirek Giersz,[1]★ Abbas Askar,[1] Nathan Leigh[3] and Arkadiusz Hypki[4]

[1]*Nicolaus Copernicus Astronomical Centre, Polish Academy of Sciences, ul. Bartycka 18, PL-00-716 Warsaw, Poland*
[2]*CAPES Foundation, Ministry of Education of Brazil, DF 70040-020 Brasilia, Brazil*
[3]*Department of Astrophysics, American Museum of Natural History, Central Park West and 79th Street, New York, NY 10024, USA*
[4]*Leiden Observatory, Leiden University, PO Box 9513, NL-2300 RA Leiden, the Netherlands*

Accepted 2016 July 25. Received 2016 July 22; in original form 2016 April 21

ABSTRACT

In this paper, which is the first in a series of papers associated with cataclysmic variables and related objects, we introduce the CATUABA code, a numerical machinery written for analysis of the MOCCA simulations, and show some first results by investigating the present-day population of cataclysmic variables in globular clusters. Emphasis was given on their properties and the observational selection effects when observing and detecting them. In this work, we analysed in this work six models, including three with Kroupa distributions of the initial binaries. We found that for models with Kroupa initial distributions, considering the standard value of the efficiency of the common envelope phase adopted in BSE, no single cataclysmic variable was formed only via binary stellar evolution, i.e. in order to form them, strong dynamical interactions have to take place. We show and explain why this is inconsistent with observational and theoretical results. Our results indicate that the population of cataclysmic variables in globular clusters is, mainly, in the last stage of their evolution and observational selection effects can drastically change the expected number of observed cataclysmic variables. We show that the probability of observing them during the outbursts is extremely small and conclude that the best way of looking for cataclysmic variables in globular clusters is by searching for variabilities during quiescence, instead of during outbursts. For that, one would need a very deep observation which could reach magnitudes $\gtrsim$27 mag. Finally, we argue that cataclysmic variables in globular clusters are not necessarily magnetic.

Key words: methods: numerical – novae, cataclysmic variables – globular clusters: general.

1 INTRODUCTION

The study of star clusters plays an important role in our understanding of the Universe since these systems are natural laboratories for testing theories of stellar dynamics and evolution. Particularly, globular clusters (GCs) are one of the most important objects for studying the formation and the physical nature of exotic objects such as X-ray binaries, degenerate binaries, black holes and blue straggler stars, which in turn provides basic information and tools that can help us to understand the formation and evolution processes of star clusters, galaxies and, in general, the young Universe.

Among the most interesting objects in GCs are the cataclysmic variables (CVs) that are interacting binaries composed of a white dwarf (WD) that accretes matter stably from a main-sequence (MS) star – or, in the last stage of their evolution, a brown dwarf (BD; e.g. Knigge, Baraffe & Patterson 2011, for a comprehensive review). CVs are subdivided according to their photometric behaviour as well as the magnetic field strength of the WD, being, mainly, magnetic CVs (where the accretion is partially or directly via magnetic field lines) and non-magnetic CVs (where the accretion is via an accretion disc). Among the non-magnetic CVs, the most prominent subgroup is that composed of dwarf novae (DNe) which exhibit repetitive outbursts due to the thermal instability in the accretion disc (e.g. Lasota 2001, for a review).

1.1 CV formation

CVs are believed to form from an MS–MS binary that undergoes a common envelope phase (CEP) when the more massive MS evolves to a giant (Paczynski 1976). In such CEP, the dense stellar giant core and the MS spiral towards each other with the expansion and loss of the common envelope. Most of the angular momentum is lost with the envelope which leads to an orbital period orders of magnitude

★ E-mail: belloni@camk.edu.pl (DB); mig@camk.edu.pl (MG)

shorter (e.g. Webbink 1984). After the CEP, a pre-CV is formed in a detached WD–MS binary. Because of angular momentum loss (see below), the separation between the stars decreases up to the formation of the CV, when the MS starts filling its Roche lobe.

In order to form a CV through the above-mentioned scenario, the initial MS–MS binary should approximately have the following properties: (i) the more massive star has $M \lesssim 10\,\mathrm{M}_{\odot}$; (ii) the less massive star is a low-mass MS; (iii) the mass ratio is $\lesssim$0.25; (iv) the separation has to be sufficient to allow the primary to expand to a point where it could form a degenerate core (pre-WD) and to permit the contact (the CEP).

The reasons for these conditions come almost naturally. The mass of the more massive star has to be in the acceptable range to form a WD. This justifies the first condition. Besides, the mass ratio after the CEP has to be $\lesssim$1 (e.g. Hellier 2001). Otherwise, the mass transfer would be unstable and such instability would precipitate further mass transfer and then a merger would occur. This is because the mass transfer rate becomes very large and the WD cannot steadily burn the accreted material, then it swells up to become a giant, producing a common envelope binary and a merger of the stars. The WD mass cannot be greater than $\sim$1.44 $\mathrm{M}_{\odot}$; thus, in order to have the mass ratio less than one, the secondary mass cannot be larger than the WD mass, after the CEP. This justifies the second condition. About the mass ratio, if the initial mass ratio is great ($q \sim 1$), then both stars will have similar evolutionary time-scales. In this way, the stars would become WDs at roughly the same time. For a CV however, one star has to be a WD and the other one an MS. This explains the reason for the third condition. Finally, if the separation was too large, the more massive star could not fill its Roche lobe. While if it was too small, the Roche lobe overfilling could lead to a merger. Then, the separation has to be ideal to allow for both the formation of a WD-like core and the close post-common envelope binary.

1.2 CV evolution

Non-magnetic CVs are usually separated in the following way, with respect to the orbital period: (i) if the donor is an MS and $P_{\mathrm{orb}} \gtrsim$ 3 h, then it is called a long-period CV; (ii) if the donor is an MS and $P_{\mathrm{min}} \lesssim P_{\mathrm{orb}} \lesssim$ 2 h, then it is called a short-period CV; and (iii) if the donor is a BD, it is called a period bouncer CV (in this case, $P_{\mathrm{orb}} \gtrsim P_{\mathrm{min}}$). Besides, in CVs (especially non-magnetic ones), angular momentum loss is the driving mechanism for their long-term evolution. In the so-called standard model of CV evolution, the dominant angular momentum loss mechanism in long-period CVs is magnetic braking (Rappaport, Joss & Webbink 1982), whereas in short-period and period bouncer CVs the driving mechanism is associated with the emission of gravitational radiation (Paczyński 1967).

Basically, two important features observed in non-magnetic CVs need to be explained by the standard model. First, the absence of systems in the range of 2 h $\lesssim P_{\mathrm{orb}} \lesssim$ 3 h, known as the period gap (e.g. Zorotovic et al. 2016, and references therein) and, secondly, the existence of a period minimum $P_{\mathrm{min}} \approx 82$ min (e.g. Gänsicke et al. 2009). The standard model reasonably fulfils its role in explaining the observational properties of the CVs.

Briefly, the standard model can be summarized as follows: after the birth of the CV, it will evolve towards short periods due to angular momentum loss. When it reaches $P_{\mathrm{orb}} \sim 3$ h (upper edge of the period gap), the donor becomes fully convective and Rappaport, Verbunt & Joss (1983) proposed that at this point the magnetic braking turns off or becomes less efficient (disrupted magnetic braking scenario). This results in a decrease of the mass transfer rate, which allows the donor star to reestablish its equilibrium and to stop filling its Roche lobe. Then, the system becomes detached since the mass transfer stops. However, such a detached WD–MS binary keeps evolving towards shorter periods due to gravitational radiation. When $P_{\mathrm{orb}} \sim 2$ h (inner edge of the period gap), the Roche lobe has shrunk enough to restart mass transfer and the system becomes a CV again. After that, at some point during its evolution ($P_{\mathrm{orb}} \sim P_{\mathrm{min}}$), the mass-loss rate from the secondary drives it increasingly out of thermal equilibrium until the thermal time-scale exceeds the mass-loss time-scale and it expands in response to the mass-loss, thus, increasing P_{orb}. Consequently, a large number of CVs are expected to be near the period minimum (known as the period spike) or be in post-period minimum phase – indeed, the abundance ratio for long-period CVs, short-period CVs and period bouncers, respectively, is roughly 1:30:70 (e.g. Howell, Rappaport & Politano 1997).

1.3 CV observation

Since the birth of interest in CVs (e.g. Warner 1995, for a historical review), several breakthroughs have been taking place in the field, especially due to the Sloan Digital Sky Survey which has provided a reasonable sample that reaches deeper magnitudes and which is capable of recognizing very faint CVs near and beyond the period minimum (P_{min}). Such breakthroughs include the confirmation of the disrupted angular momentum loss at the period gap (Zorotovic et al. 2016), the discovery of period bouncers with BD donors (Littlefair et al. 2006), the discovery of the period spike around P_{min} (Gänsicke et al. 2009), among others. They allowed the community to considerably improve the observational data to confront theoretical predictions which, in turn, have led to a stronger corroboration between theory and observation.

All the previous discussions, theoretical and observational, are mainly concerned with CVs in the field. For CVs in GCs, the same is not always true because of the influence of dynamical interactions, the ages and distances of the GCs, and the corresponding observational selection effects. Some observational efforts have also been made regarding CVs in GCs, especially a search for an optical counterpart of *Chandra* X-ray observations (e.g. Knigge 2012, for a review on CVs in GCs).

In general, there are four main approaches that have been used for detecting CVs in GCs. In what follows, we will describe them briefly including also the few important works associated with them.

1.3.1 Variability during outbursts

In all possible sorts of variability related to CVs, the most explored is that regarding the DN outbursts which last from days to tens of days and result in an increase of luminosity by roughly 2–5 mag.

The first major investigation of CVs in GCs was done by Shara et al. (1996), who analysed 12 epochs of *Hubble Space Telescope* (*HST*) observations of the GC 47 Tuc and recognized only one DN and one DN candidate. Other DNe have been discovered through variability during outbursts after that in different clusters (e.g. Shara, Hinkley & Zurek 2005; Knigge et al. 2003; Servillat et al. 2011). In a survey-like search for DNe, Pietrukowicz et al. (2008) analysed 16 Galactic GCs and yielded two new certain DNe: M55-CV1 and M22-CV2. They found that the total number of known DNe in the Galactic GCs is 12 DNe, distributed among seven clusters.

Some comments are needed at this point. As Knigge (2012, see section 5.5) has already pointed out, both Shara et al. (1996) and Pietrukowicz et al. (2008) concluded that DNe are rare in GCs based on the properties of observed CVs in the Galactic field, which seems to be a biased sample of the real population of CVs in the field. If most CVs in the field are, in fact, period bouncers, then the observed CV population in the field (especially the bright ones) is not representative of the real population of CVs in the Galactic field. This is mainly due to the very small duty cycle (fraction of the DN cycle that a DN is in outburst) associated with period bouncers. Hence, in this case, most CVs in the field are unobservable at any given time, and a significant population of hidden CVs exists. Thus, the conclusion that DNe are rare in GCs is not necessarily correct, since it could just be that they are hard and/or unlikely to observe, since there are more period bouncer CVs than originally expected (Knigge 2012).

Therefore, it turns out that identifying CVs through their variability during outbursts is unlikely to reveal the intrinsic population of CVs in GCs since one should be very lucky to detect the outbursts in a sequence of epochs from *HST*, given the extremely small duty cycle associated with the CVs in GCs.

1.3.2 Hα imaging

Another possible way to detect CV candidates is using Hα imaging (e.g. Cool et al. 1995), since systems that exhibit an excess in Hα show evidence of variability. This technique is generally used to study the counterparts of X-ray sources and has revealed few CVs in some GCs (e.g. Grindlay 2006; Pietrukowicz 2009). However, doubt remains about the deepness of observations using these techniques, i.e. if they are able to detect the faint population of CVs in GCs.

So far, Cohn et al. (2010) have reached magnitudes as deep as 28 for Hα and 26 from optical observations of the *HST*. Their study seems to be the least affected by this kind of bias and will be used in this paper as the object for comparison with our results.

1.3.3 FUV band with HST

Another way to detect potential CVs is through their colours. CVs tend to be bluer due to accretion processes. In fact, the energy released from this mechanism makes the region close to the WD hotter, which in turn makes the CVs bluer than typical stars in GCs.

This implies that looking for them in the far-ultraviolet (FUV) band with *HST* is a good way to find CV candidates (e.g. Dieball et al. 2010). Especially because most MSs in GCs emit in infrared which nulls the problem with crowding.

Dieball et al. (2010) carried out a detailed search in the core of M80 and found few candidates. However, due to their limiting magnitude, they could only detect bright CV candidates. In this way, the detection of the faint CVs using the *HST*'s FUV detectors might also be problematic.

1.3.4 X-rays

The high resolution that has been achieved with *Chandra* allows us to, in fact, reach binaries with compact objects in GCs, especially in their cores.

With regard to CVs, many GCs have been studied with *Chandra* down to $\sim 10^{32}$ erg s^{-1} (e.g. Pooley 2010). Additionally, the identification of optical counterparts with deep *HST* imaging has allowed for the recognition of many CV candidates (e.g. Bassa et al. 2004; Cohn et al. 2010; Huang et al. 2010), although the number of such candidates is far from the predicted number of CVs in the observed clusters.

Finally, it is valid to note that below $\sim 10^{32}$ erg s^{-1}, a large fraction of X-ray sources do not have secure optical counterparts. Below this value, the sources can be chromospherically active binaries (or near-contact binaries of MSs), CVs, foreground and background objects, quiescent low-mass X-ray binaries, millisecond pulsars or black hole X-ray binaries. Any conclusions drawn from a comparison between the results of our simulations and observations of CVs with small X-ray luminosities should be taken with a grain of salt. This is because the observational sample can be regarded as something of an upper limit, due to an increased probability of contamination from active binaries, chromospherically active stars, accreting neutron stars and black holes, etc.

1.3.5 Classical novae

On the subject of classical novae (CVs with high mass transfer rates and stable and hot discs), it is worth mentioning some observational evidence of different nova rates with respect to the Galactic field.

Curtin et al. (2015) detected novae in a survey of GCs in three Virgo elliptical galaxies (M87, M49 and M84). Such a survey should not detect any novae if there were no enhancement of the nova rate due to dynamics.

A similar result was reached by Shara et al. (2004) while investigating one GC of M87. They concluded that classical nova eruptions in GCs are up to 100 times more common than current detections in the Milky Way suggest.

This implies that dynamics are extremely important in enhancing the detection rate of novae in GCs.

1.3.6 What is the lesson from the observations?

Given the crowding of GCs and the faintness of the intrinsic population of CVs, confirming spectroscopically the many CV candidates that have been observed as real CVs is challenging (e.g. Knigge et al. 2003; Thomson et al. 2012). On the other hand, the usage of a combination of different techniques (Hα and FUV imaging, X-ray, colour, etc.) can provide almost guarantees the confirmation of CVs, especially for DNe. For instance, Cohn et al. (2010) used Hα imaging and colours to infer that some *Chandra* X-ray sources are CVs.

As it seems, a combination of techniques can provide us with the potential number of CVs in GCs. The only problem is whether or not we can reach faint CVs, given the observational limitations and biases of each technique when combined together.

This indicates that the biases and observational limitations can lead us to incorrect impressions about the nature of CVs in GCs.

1.4 Nature of CVs in GCs

In the most recent survey-like search for DNe, Pietrukowicz et al. (2008) conclude that 'ordinary DNe are indeed very rare in GC'. Then, either the predicted number of CVs is not correct or the predicted CVs would be non-DNe. Nevertheless, such observational findings do not corroborate theoretical predictions.

First, theoretical works predict that most CVs should be DNe (e.g. Knigge et al. 2011). Secondly, some previous numerical investigations regarding CVs in evolving GCs estimate around 100–200 CVs in massive GCs. In the most recent study on the matter, Ivanova et al. (2006) predicted that around 200 CVs would be present in a

typical massive GC. Besides, such CVs would have different properties from the CVs in the field. For example, only ∼25 per cent of CVs were formed in binaries that would become CVs in the field. Also, approximately 60 per cent of the CVs did not form via a CEP.

This corresponds to a rather strong inconsistency between theory and observation, and the most popular hypothesis that attempts to explain the so-called absence of DNe in GCs is based on the mass transfer rate and the WD magnetic field. Dobrotka, Lasota & Menou (2006) proposed, using the disc instability model (DIM), that a low mass transfer rate combined with a moderately strong WD magnetic field can disrupt the inner part of the disc, preventing, in turn, an outburst in such CVs.

In the mid-1990s, the community started to think that CVs in GCs tend to be magnetic due to the work by Grindlay et al. (1995) who analysed three CVs in NGC 6397 and found the existence of He II line in such CVs. Also, Edmonds et al. (2003a,b) argued in the same direction in their studies of 47 Tuc.

The big problem with this argument is that not only magnetic CVs exhibit the He II line in their spectra, but also other types of CVs (Knigge 2012). For instance, Shara et al. (2005) found DN-like eruptions in CV2 and CV3 in NGC 6397 which exhibited helium emission in their spectra. Therefore, it seems that such evidence is not strong enough to claim that CVs in GCs are, principally, magnetic ones.

The main reason for this suspicion is the attempt to explain the discrepancies between observed CVs in GCs and those in the field. This is because a WD magnetic field can prevent instability in the disc and, in turn, suppress the occurrence of outbursts (Dobrotka et al. 2006). Besides, it could explain to some extent the unique X-ray and optical properties found for the CVs in GCs.

However, the CV samples in GCs tend to be X-ray selected (Heinke et al. 2008) which, in turn, favours the detection of magnetic CVs (brighter in X-ray than the non-magnetic counterpart). Unfortunately, few investigations went deep enough to detect the non-magnetic CVs ($\lesssim 10^{30}$ erg s^{-1}) in the X-ray, and more efforts should be put in this direction.

Another point in favour of the idea that CVs in GCs are magnetic comes from the fact that magnetic CVs are usually associated with massive WDs (Ivanova et al. 2006). In fact, in GCs, the dynamically formed CVs tend to have higher WD masses which, in turn, favours the hypothesis of magnetic CVs.

Above all, such a hypothesis is not well established and can be contested. As has already been mentioned, most CVs should be DNe (Knigge et al. 2011). Besides, not only magnetic CVs produce the above-mentioned He II emission. Over and above, many optical counterparts of X-ray sources have been recognized as reasonable CV candidates in some GCs (e.g. Cohn et al. 2010), although such numbers are still far from the predicted number of CVs.

1.5 Structure of the paper

From the last subsection, we can say that the 'CV problem in GCs' is not yet well understood and solved. In order to contribute to such a discussion, this is the first paper of a series that concentrates on CVs and related objects (such as AM CVn and symbiotic stars) in evolving GCs that attempt to correlate CV properties (and also AM CVn and symbiotic star properties) with cluster initial and present-day parameters.

The main objective of this first paper is to introduce the CATUABA code (Section 3) that will be used in this series of papers to derive properties of CVs and related objects from MOCCA simulations. In order to test its efficiency and coherence, we concentrate on only six models with different initial conditions and different properties at the present day (described in Section 4). The models were simulated by the MOCCA code (Section 2) that simulates real GCs on a time-scale of one day. Its speed allows for the simulation of hundreds of models in a short time and, in turn, permits a very detailed statistical analysis of particular objects (like CVs) and their correlations with the cluster parameters. The aim of this series of papers is to analyse the MOCCA data base with respect to CVs and related objects.

For convenience, we decided to separate the results of this initial work into two separate papers. In this paper, we will concentrate mainly on the present-day (considered here as 12 Gyr) population of CVs present in the analysed models. In the next, we will discuss mainly the CV progenitors and the main formation channels as well as their properties at the moment they are formed and the subsequent evolution up to present day. We will also deal with more general issues like unstable systems, escaping binaries that become CVs, and so on.

In Section 2, we describe the MOCCA and BSE codes. We also make some comments with regard to the comparison between MOCCA and *N*-body codes. We describe the CATUABA code in Section 3, and end the section by summarizing its main features. The models used in this first work will be described in Section 4, and in Section 5, the main results of the preliminary investigation are presented. We show results associated with the clusters and their present-day populations (PDPs) of CVs as well as results related to observational selection effects when searching for CVs in GCs. We also address some connections between our results and observations and, also, between our investigation and previous studies. We conclude and discuss the main implications of these first results in Section 6. Finally, throughout this paper, we use some new abbreviations, and for convenience, in Appendix A, we clearly define all abbreviations in order to allow the reader to consult them if necessary.

2 MOCCA CODE

In this section, we describe the MOCCA code that was used to simulate the cluster evolution. We also describe the BSE code that is utilized by MOCCA to perform the stellar evolution. We end this section by briefly comparing MOCCA's performance with that of *N*-body codes.

The MOCCA code (Hypki & Giersz 2013; Giersz et al. 2013, and references therein) is based on the orbit-averaged Monte Carlo technique for cluster evolution developed by Hénon (1971), which was further improved by Stodółkiewicz (1986). It also includes the FEWBODY code, developed by Fregeau et al. (2004), to perform numerical scattering experiments of gravitational interactions. To model the Galactic potential, MOCCA assumes a point mass with total mass equal to the enclosed Galaxy mass at the Galactocentric radius. The description of escape/capture processes in tidally limited clusters follows the procedure derived by Fukushige & Heggie (2000). The stellar evolution is implemented via the SSE code developed by Hurley, Pols & Tout (2000) for single stars and the BSE code developed by Hurley, Tout & Pols (2002) for binary evolution.

2.1 BSE code

The most important part of MOCCA with regard to CVs and related objects is the BSE code (Hurley et al. 2002). BSE models angular momentum loss mechanisms, although its implementation is not up-to-date (Knigge et al. 2011, for a revised model). Mass transfer occurs if either star fills its Roche lobe and may proceed on a nuclear, thermal or dynamical time-scale. Prescriptions to determine the type and rate of mass transfer and the response of the primary to accretion

are implemented in BSE. The overall CV evolution can be recovered by BSE, although some comments are necessary here.

With respect to the CEP, BSE assumes that the common envelope binding energy is that of the giant(s) envelope involved in the process. In order to reconcile the prescription developed by Iben & Livio (1993), we use the recommended value for the CEP efficiency which is 3.0. This is greater than the usually adopted values, but we kept it for the initial investigation.

With respect to CV evolution, the donor radii for long-period CVs are not increased in BSE. There is observational evidence of an increase in the radii of CV donors with radiative cores (Knigge et al. 2011, see their fig. 6). Besides, the mass transfer rate is not adjusted to be in agreement with those derived from observations in the field. This implies a different CV evolution, which leads to the absence of the period gap and to a different period minimum. Additionally, for period bouncers, the mass–radius relation leads to a faster increase in the period after the period minimum.

Even though some efforts should be put into the improvement of BSE in this direction, for the purposes of this work, the approach already implemented in BSE seems reasonable. Furthermore, we use standard values for all parameters in the BSE code (Hurley et al. 2002) None the less, we have to bear in mind these factors while analysing the results.

2.2 Comparison with *N*-body codes

MOCCA was extensively tested against *N*-body codes. For instance, Giersz et al. (2013) concluded that MOCCA is capable of reproducing *N*-body results with reasonable precision, not only for the rate of cluster evolution and the cluster mass distribution, but also for the detailed distributions of mass and binding energy of binaries. Additionally, Wang et al. (2016) also compared MOCCA with the state-of-the-art NBODY6++GPU and showed good agreement between the two codes.

In general, many of the simplifying assumptions adopted in the Monte Carlo method that would be naturally accounted for in an *N*-body code are unimportant in the regime of cluster masses where Monte Carlo models are ideally suited. For example, Monte Carlo methods treat both binary evolution and direct single–binary and binary–binary encounters as isolated processes, with no chance of being interrupted due to a dynamical encounter. This was recently shown to be a valid assumption in clusters more massive than $\gtrsim 10^5$ $M_\odot$, with the probability of interruption being of the order of a per cent or less (Geller & Leigh 2015; Leigh, Geller & Toonen 2016). The approximations underlying the Monte Carlo method are in many ways perfectly suited to model massive cluster evolution, the regime of star cluster evolution where *N*-body models cannot typically go (at least not without being severely limited by the computational expense).

In essence, MOCCA is ideal for performing big surveys and for carrying out detailed studies of different types of objects like CVs (this paper), blue straggler stars (Hypki & Giersz 2013, 2016a,b), intermediate-mass black holes (Giersz et al. 2015), X-ray binaries, etc., and provides good agreement with *N*-body codes.

2.3 Why MOCCA?

The MOCCA code has been developed for more than 20 years (Giersz 1998, 2001, 2006; Giersz, Heggie & Hurley 2008), and its current version (Giersz et al. 2013; Hypki & Giersz 2013) is characterized by its high speed, its modularity and its detailed information about each and every object in the system.[1]

In this way, MOCCA is convenient for two purposes that will help with the investigation of CVs and related objects in GCs: (i) its high speed allows for generating a big data base covering a huge range in the cluster parameter space and subsequently allows for powerful statistical analysis regarding the cluster parameters and the studied objects; (ii) its list of the most relevant events during the life of each star in the cluster admits a very detailed investigation concerning formation/destruction channels, strength of dynamical interactions, and so on.

To sum up, the MOCCA code is ideal for performing big surveys and for carrying out detailed studies of different types of exotic objects like CVs, blue straggler stars, degenerate binaries, etc.

2.4 The MOCCA-SURVEY data base

Askar et al. (2016, see their table 1) describes the set of 1950 GC models (called MOCCA-SURVEY) that were simulated using the MOCCA code. The models have quite diverse parameters describing not only the initial global cluster properties, but also star and binary parameters.

The clusters vary with respect to (i) metallicity: 0.02, 0.006, 0.005, 0.001 and 0.0002; (ii) binary fraction: 0.95, 0.3, 0.1 and 0.05; (iii) King model parameter (W_0): 9.0, 6.0 and 3.0; (iv) tidal radius: 120.0, 60.0 and 30.0; (v) cluster concentration as measured by the ratio between tidal and half-mass radii: 50.0, 25.0 and tidally filling; (vi) initial binary properties (period, eccentricity and mass ratio), being the initial mass function (IMF) given by Kroupa (2001); (vii) supernova natal kicks for black holes distributed according to Hobbs et al. (2005) or reduced according to mass fallback description given by Belczynski, Kalogera & Bulik (2002).

Despite the fact that the models in the MOCCA-SURVEY were not selected to match the observed Milky Way GCs, they agree well with the observational properties of the observed GCs (Askar et al. 2016, see their fig. 1). They conclude that the MOCCA-SURVEY cluster models are representative for the Milky Way GC population. The six models discussed in the paper were chosen from the MOCCA-SURVEY data base.

3 CATUABA CODE

In this section, we describe the code CATUABA[2] (Code for Analysing and sTUdying cAtaclysmic variables, symBiotic stars and AM CVns), which is capable of investigating CVs. In future improvements, it will be extended to also include symbiotic stars and AM CVn.

First, we describe how the CATUABA code recognizes the PDP in clusters simulated by MOCCA and also how it separates the CVs according to their main formation mechanisms. Secondly, we explain the main physical assumption included in the code to study the observational properties of the PDP of CVs in a simulated cluster. Thirdly, we describe other features included in the code and finish

[1] The simulations were performed on a PSK cluster at the Nicolaus Copernicus Astronomical Centre in Poland.

[2] Catuaba is a vigorous-growing, small tree that produces yellow and orange flowers and small, dark yellow, oval-shaped, inedible fruit. It grows in the northern part of Brazil, the Amazon, Para, Pernambuco, Bahia, Maranhao and Alagoas. Catuaba has origin in one Brazilian indigenous language (tupi-guarani) and means ‘strong plant’ since its bark tea is a central nervous system stimulant and also an innocent aphrodisiac.

the section with a summary of its operation based on a flow chart of its prime provisions for the analysis of the CV population.

3.1 CV populations

In this subsection, we describe the three populations used to study the CVs. They correspond to the properties of the same CVs at three different times.

3.1.1 The present-day population

The first step in the construction of an inventory of CVs in a GC is the recognition of their population at the present-day age of such a cluster. This is possible due to recurrent snapshots (around every 200–250 Myr) of the system recorded by MOCCA during the simulation. We have chosen a snapshot of the cluster at around 12 Gyr to be the present-day cluster. Then, an extraction of the PDP of CVs is easy, based on the definition given in Section 1.

Once the stars in the PDP of CVs are recognized, a complete study of them is done from the progenitor population (see below) up to the PDP. MOCCA provides a full history of the dynamical and physical evolutionary events of all stars in the system (Hypki & Giersz 2013, for blue straggler stars) through the MOCCA-MANAGER code.

3.1.2 The progenitor and formation-age populations

Given a star in the cluster, MOCCA-MANAGER creates a complete history of all relevant steps during the life of the star thereof. In this chronological list, all stellar evolution and dynamical events are recorded. Therefore, we can easily get the properties of the progenitor population and the formation-age population of CVs in the cluster. The progenitor population is defined here as the population of all binaries that are progenitors of the PDP of CVs, i.e. the population of CVs at the birth of the cluster.

Now, the formation-age population is the population related to the birth of the CV itself, in the sense that mass transfer starts from MS on to a WD. Obviously, for the formation-age population, the time is not unique as in the progenitor population and the PDP. During the cluster evolution, each CV is formed at a specific time, different from the other ones.

One comment about dynamical exchanges and the progenitor population of CVs is necessary at this point.

First, we define a dynamical exchange (or just exchange) by a process in which a binary has one of its components replaced by another star in a binary–single or a binary–binary interaction. It can happen (and happens) that a CV can be formed due to exchanges, in the sense that both the CV components are not the same as those of the primordial binary.

Secondly, the progenitor population of CVs for the cases without exchange is easily determined, since the components of the primordial binary are the same components of the CV. Although the situation is not straightforward when there is exchange in the history of the CV. The initial properties in the case of exchange are obtained by getting the properties of the binary with the smaller period (if the exchange took place in a binary–binary interaction) or the properties of the binary (if the exchange happened in a single–binary interaction). In the case that both components of the CV in the PDP were single stars at the cluster birth, then such CVs are excluded from the progenitor population since there is no initial binary associated. In summary:

(i) if both CV components are the same at the very beginning, then the CV is formed from the primordial binary, i.e. there is no exchange during the binary's life. Thus, this binary enters into the progenitor population;

(ii) if one CV component comes from one binary and the other one comes from another binary, then the properties of the binary with the smaller size at the beginning is saved in the progenitor population;

(iii) if one CV component comes from a binary and the other one was a single star at the very beginning, then the binary properties are saved in the progenitor population;

(iv) if both CV components come from single stars, then there is no binary at the very beginning associated with the CV. Since the progenitor population is defined for binaries only, we do not include any binary for such a CV in the progenitor population.

It is worthwhile to mention that only a few CVs enter in case (iv) above (<1 per cent for the models investigated here) which, in turn, will not change the conclusion derived from the analysis of the progenitor population (in the second paper).

3.2 Categorization of the present-day CVs

Given the complete history of events during the lives of the CVs in the PDP, an attempt of categorizing them comes naturally. Our choice was to separate them with respect to the importance of the dynamical interactions in their lives. For that, we separate every CV in one of the following groups: (i) *Binary stellar evolution group (BSE group)*: the formation of the CV and its subsequent evolution was *without* any influence of dynamical interactions. This means that a CV in this group has formed from a binary in the progenitor population *only* through binary stellar evolution. (ii) *Weak dynamical interaction group (WDI group)*: the CV life was influenced only by *weak* dynamical interactions, in the sense that the binding energy during such interactions changes by a factor of less than 20 per cent during the evolution of the binary in the progenitor population up to the formation of the CV and subsequently, up to PDP. (iii) *Strong dynamical interaction group (SDI group)*: the formation of the CV was influenced *strongly* by dynamical interactions, in the sense that such interactions have significantly changed the evolution of the binary in the progenitor population up to the formation of the CV. After the formation of the CVs in this group, there are no subsequent strong dynamical interactions.

Some comments are worthwhile to mention before proceeding further.

(i) Whether a CV belongs to the WDI group or the SDI group is a priori arbitrary. It is based on the change of energy during the dynamical interactions. The cutoff between a weak dynamical interaction and a strong one is 20 per cent of the initial binding energy. This cutoff is for only one dynamical interaction, and it is an arbitrary value connected to the average energy change according to Spitzer's formula for equal-mass systems (Spitzer 1987). Generally, for weak dynamical interactions, most of the interactions are fly-bys, although they can also be resonant interactions, and for strong dynamical interactions, they can be resonant or exchange interactions. As follows, if a binary undergoes one interaction and the change of its binding energy is less than 20 per cent, this binary was involved in one weak dynamical interaction; otherwise, it was subjected to one strong dynamical interaction. If a binary underwent *only* weak dynamical interactions during its life, then this binary belongs to the WDI group. Now, if a binary underwent *at least one*

strong dynamical interaction in its life, then this binary belongs to the SDI group.

(ii) The WDI group is formed by CVs which had only weak encounters during their lives. However, if the number of these encounters is high for a CV in this group, their cumulative effect can be strong and the properties of the progenitor binary can be strongly changed during its life. Otherwise, if the cumulative effect of the weak dynamical interactions is not strong, the CV will probably have similar properties to those belonging to the BSE group.

(iii) The SDI group also includes binaries which underwent either exchange or merger.

3.3 CV properties

In this part of the methodology, we provide the main assumptions related to the CV properties. We state the main theoretical and empirical relations used in CATUABA. With such properties, we can estimate an upper limit for the probability of observing a CV (Section 3.4).

Once the PDP of the CVs is acquired, we can start to analyse the properties of the population thereof. Fortunately, the BSE code in MOCCA is capable of giving basic information about binaries in snapshots of the cluster, like masses, orbital elements, bolometric luminosities, radii and magnitudes. None the less, in the precise case of CVs, BSE is not able to model the typical behaviours of sub-types of CVs, including DIMs. These processes need to be covered in our analysis.

This is necessary because one of the aims of the CATUABA code is to calculate the probability of observing CVs as a function of the GC distance and the optical limiting magnitude. Besides, it is rather important to have a model of how the brightness varies with time for systems that undergo variability (like CVs). In the specific case of CVs, the variability is caused by either eclipses or outbursts, and the chances of detecting a CV depend on how its magnitude varies with time due to either eclipses or recurring outbursts. In order to compute such brightness variations due to outbursts, the well-accepted DIM will be used as it provides maximum values for the CV luminosity during quiescence and during outburst.

3.3.1 CV types

As we have already mentioned, one expects that most CVs are DNe (Knigge et al. 2011). In this sense, we should be able to model DNe.

DNe are characterized by outbursts due to the thermal instability in the accretion disc (e.g. Smak 2001). During the outburst, their luminosity increases by typically 2–5 mag. Also, outbursts last from days to tens of days, and occur every tens of days or even decades.

In order to classify a CV as a DN, we adapted equations A.3 and A.4 of Lasota (2001) which defines the limits for the disc stability based on the CV properties, the position inside the disc and the viscosity parameter α. Hence, the mass transfer rate $\dot{M}_{\rm B}$ defines the limit between hot/ionized/stable and unstable disc, and the mass transfer rate $\dot{M}_{\rm A}$ defines the limit between cold/neutral/stable and unstable disc. They are

$$\dot{M}_{\rm A} = 6.344\times10^{-11}\,\alpha_{\rm c}^{-0.004}\left(\frac{M_{\rm WD}}{\rm M_\odot}\right)^{-0.88} \times\left(\frac{r}{10^{10}\ {\rm cm}}\right)^{2.65}{\rm M_\odot\ yr^{-1}} \quad (1)$$

and

$$\dot{M}_{\rm B} = 1.507\times10^{-10}\,\alpha_{\rm h}^{0.01}\left(\frac{M_{\rm WD}}{\rm M_\odot}\right)^{-0.89} \times\left(\frac{r}{10^{10}\ {\rm cm}}\right)^{2.68}{\rm M_\odot\ yr^{-1}} \quad (2)$$

where $M_{\rm WD}$ is the WD mass, $\alpha_{\rm c}$ is the usual viscosity parameter for the cold branch of the Shakura & Sunyaev (1973) solution, adopted here as 0.01, $\alpha_{\rm h}$ is the usual viscosity parameter for the hot branch of the Shakura–Sunyaev solution, set here as 0.1, and r is the radial distance from the centre of mass. At each r, $\dot{M}_{\rm A}$ is the critical mass transfer rate below which the disc is cold/neutral and stable and $\dot{M}_{\rm B}$ is the critical mass transfer rate above which the disc is hot/ionized and stable.

Both values ($\dot{M}_{\rm A}$ and $\dot{M}_{\rm B}$) are computed based on analytic fits concerning 1D time-dependent numerical models of accretion discs, using an adaptive grid technique and an implicit numerical scheme, in which the disc size is allowed to vary with time (Hameury et al. 1998).

Given the mass transfer rate of a CV in the PDP ($\dot{M}_{\rm tr}$), we have three different regimes: (i) if $\dot{M}_{\rm tr} > \dot{M}_{\rm B}$ everywhere in the disc, the disc is stable and hot; (ii) if $\dot{M}_{\rm tr} < \dot{M}_{\rm A}$ everywhere in the disc, the disc is stable and cold; (iii) if $\dot{M}_{\rm A} < \dot{M}_{\rm tr} < \dot{M}_{\rm B}$, in some ring r of the disc, the disc is unstable and undergoes repetitive outbursts.

3.3.2 Mass transfer and accretion rates

Before moving on, we have to explain how the mass transfer and accretion rates are calculated, since this information is not given by the BSE code in MOCCA. The *mass transfer rate* here is defined as the mass-loss rate of the donor, i.e. the rate at which the accretion disc is fed (in the case of a non-magnetic CV or an intermediate polar CV). On the other hand, the *accretion rate* is defined as the rate at which the mass flows through the accretion disc towards the WD.

It is worth noticing that in long-period CVs in which the donor is an evolved star (sub-giant), the mass transfer can also be driven by the nuclear expansion of the donor star, e.g. AKO 9 in 47 Tuc (Knigge et al. 2003). Nevertheless, based on our definition of CV (Section 1), we are mainly concerned with unevolved donors, which is reasonable, since MS stars are more common in GCs than more evolved donors by orders of magnitude.

On how the mass transfer rate is computed, for simplicity, let us consider only one CV. From the list of all relevant events during the CV life, two quantities are used to compute the mass transfer rate, namely time and donor mass. For each timestep in the CV life, the mass transfer rate is computed based on the amount of mass lost by the donor due to angular momentum loss during this timestep. Thus, the mass transfer rate calculated here corresponds to a crude estimation. The accretion rate will be treated latter in this section.

We assume, a priori, that the disc is not disrupted and the inner edge of the disc is the WD radius. Besides, the outer edge of the disc during outbursts is assumed to be 90 per cent of the WD Roche lobe (Smak 1999) which, in turn, is computed based on the equation derived by Eggleton (1983).

With these values for the viscosity parameter and edges of the disc, it is straightforward to distinguish between stable and unstable discs by using equations (1) and (2).

In order to calculate the observational properties of the CVs with unstable discs, we need to find the associated accretion rates ($\dot{M}_{\rm d}$) through the disc, specifically during outburst ($\dot{M}_{\rm dO}$) and during quiescence ($\dot{M}_{\rm dQ}$).

The BSE code inside MOCCA is capable of giving some information about the binary itself. Nevertheless, information about the other components (hotspot and disc) for a DN is missing. Therefore, we adopt maximum values for the accretion rate during quiescence and outburst. For the accretion rate during quiescence, we simply assume $\dot{M}_{\rm dQ} = \dot{M}_{\rm A}$, while for the outburst, we adopt $\dot{M}_{\rm dO} = \dot{M}(d)$, where $\dot{M}(d)$ is obtained from equation 3.27 of Warner (1995), which is qualitatively similar to the expression derived by Lasota (2001).

We choose to use the maximum values during quiescence and during outburst because we are interested in an upper limit for the probability of observing a CV. A similar approach for the accretion rate is used in the STARTRACK code (Belczyński et al. 2008) which deals with X-ray binaries.

Concerning the disc radius for a DN in quiescence, we adopt a value of 50 per cent of the WD Roche lobe for the outer edge (Harrop-Allin & Warner 1996). While for the outburst, as we have already mentioned, we use a value of 90 per cent of the WD Roche lobe (Smak 1999).

3.3.3 CV visual luminosity

The WD and donor bolometric luminosities are provided by the BSE code. We only need additional information about the hotspot and the disc. The bolometric luminosity of the hotspot $L_{\rm bHS}$ is given by (e.g. Warner 1995, p. 83)

$$L_{\rm bHS} = \left(\frac{f}{8}\right) \frac{G\, M_{\rm WD}\, \dot{M}_{\rm tr}}{r_{\rm d}}, \quad (3)$$

where $f \sim 1.0$ is an efficiency factor, and the bolometric luminosity of the disc $L_{\rm bd}$ is given by (Paczynski & Schwarzenberg-Czerny 1980)

$$L_{\rm bd} = \frac{G\, M_{\rm WD}\, \dot{M}_{\rm d}}{2 r_{\rm d}} \left[1 - 3\left(\frac{R_{\rm WD}}{r_{\rm d}}\right) + 2\left(\frac{R_{\rm WD}}{r_{\rm d}}\right)^{\frac{3}{2}}\right] \quad (4)$$

with $r_{\rm d}$ being the outer edge of the disc and $R_{\rm WD}$ being the WD radius.

Once the bolometric luminosities are computed, CATUABA calculates the bolometric correction for the hotspot and for the disc. The hotspot bolometric correction is computed assuming an ellipsoid, with the semi-axes $s_{\rm a} = 0.043\ a$ and $s_{\rm b} = 0.22\ s_{\rm a}$, where a is the semi-major axis (Smak 1996). Given the shape of the hotspot and using the bolometric correction coefficients given by Torres (2010), the code computes the hotspot temperature and also the visual luminosity and magnitude.

A similar procedure is done for the disc, although it is necessary to integrate over the entire spatial extent of the disc. This is done following the procedure by Paczynski & Schwarzenberg-Czerny (1980) and also using the bolometric correction coefficients given by Torres (2010).

3.3.4 CV X-ray luminosity

Another important observational property calculated by the CATUABA code is the X-ray luminosity. This is computed based on equation 4 derived by Patterson & Raymond (1985), in the band [0.5–10 keV], for a slowly rotating WD:

$$L_{\rm X} = \varepsilon \frac{G\, M_{\rm WD}\, \dot{M}_{\rm dQ}}{2\, R_{\rm WD}}, \quad (5)$$

where the factor $\varepsilon = 0.5$ is the correction for the fraction of the X-rays emitted inwards and absorbed by the WD.

Patterson & Raymond (1985) proposed an explanation for the origin of the X-ray luminosity in CVs. They showed that, at small accretion rates (during quiescence for DNe), the boundary layer (region between the accretion disc and the WD) is the likely site of most of the observed hard X-rays. This is because at small accretion rates the boundary layer is thin. In the case of high accretion rates (during outbursts for DNe), the boundary layer is thick and consequently the observed hard X-rays do not come from this region (Eze 2015). Actually, one of the open questions on this matter is associated with the origin of the hard X-ray luminosity observed for systems with high accretion rate (Mukai et al. 2014). As there is no consensus with respect to systems with high accretion rate, equation (5) is used only for the quiescent stage (for DNe) or for CVs with stable and cold discs. There is no X-ray luminosity for the DNe during outbursts or CVs with stable and hot discs modelled in CATUABA. That is the why in equation (5) the $\dot{M}_{\rm dQ}$ is given by its value in the boundary layer, assumed here as being the WD radius.

3.3.5 DN time-scales

Important time-scales for DNe are the recurrence time and the duration of the outbursts. The recurrence time can be defined as the interval between two outbursts and is computed here based on the observational fit done by Patterson (2011)

$$t_{\rm rec} = 318 \left(\frac{M_{\rm donor}/M_{\rm WD}}{0.15}\right)^{-2.63} \ {\rm d}, \quad (6)$$

where $M_{\rm donor}$ is the donor mass and $M_{\rm WD}$ is the WD mass. Notice that the smaller the mass ratio, the longer the recurrence time.

The duration of the outburst is the interval between the beginning and the end of the outburst, and we adopt here the observational fit from Smak (1999)

$$t_{\rm dur} = 2.01\ (P_{\rm orb})^{0.78} \ {\rm d}, \quad (7)$$

where $P_{\rm orb}$ is the orbital period. Note that the longer the orbital period, the longer the duration of the outburst.

3.3.6 CVs with stable discs

Since not all CVs are DNe, the CATUABA code also has to be able to deal with systems that have stable discs. Now, we describe what happens in these cases. In stable (hot or cold) discs, it happens that the mass transfer rate is identical to the accretion rate. We adopt the maximum values in both cases, again using the prescription given by Lasota (2001) and Warner (1995), i.e. for stable and cold discs, we use $\dot{M}_{\rm A}$, and for stable and hot discs, we use $\dot{M}(d)$. Then, the same procedure is executed for computing the luminosities and the bolometric correction. Obviously, computations for the recurrence time and duration of the outburst are not necessary.

3.4 Probability of detecting a CV

One of the objectives of this work is to compute the probability of detecting a DN when observing a given GC at a distance $R_{\rm GC}$ associated with a given optical limiting magnitude $m_{\rm lim}$.

For that, let us first consider two principal configurations: (i) the CV can be detected by an optical detector/telescope in quiescence; (ii) the CV can be detected by an optical detector/telescope in outburst.

Accordingly, we can have combinations of these two cases. Thereby, the chances of observing a given CV will change based on

such a combination. Given a distance R_{GC} and a limiting magnitude m_{lim}, the probability (P_{obs}) can simply be taken from the following. If the source can be detected only during outburst, then $P_{obs} = P_O(t_{dur}, t_{rec}) = t_{dur}/t_{rec}$ is the probability of detecting the outburst in one night[3]. If the source can be detected during quiescence and during outburst, then $P_{obs} = P_{ecl} + P_O(t_{dur}, t_{rec}) = 1/3 + t_{dur}/t_{rec}$ is the probability of detecting such a CV, during the eclipse or during outburst, in one perfect night, where P_{ecl} is the probability of a CV being an eclipsing one. Finally, if the CV cannot be detected even during outburst, then the probability is null.

Notice that we are assuming that the only way to detect a CV during quiescence is when the stars eclipse each other. That is the why we add the $1/3$ term in the expression for the probability which corresponds to the probability of a binary being an eclipsing one (e.g. Hurley et al. 2002, see appendix A2 for a demonstration).

In summary, we have the following law for the probability of detecting a DN during its cycle:

$$P_{obs} = \begin{cases} t_{dur}/t_{rec}, & \text{if the CV can be observed only during outburst} \\ 1/3 + t_{dur}/t_{rec}, & \text{if the CV can be observed during quiescence} \\ 0, & \text{otherwise.} \end{cases} \quad (8)$$

It is worth explaining some issues associated with the probability expressed in equation (8). We are not considering many of the observational difficulties associated with observing a GC, like its intrinsic characteristic of being in a crowded field, a reduced number of (good) nights dedicated to observing the GC thereof, instrumental problems, etc.

Since the probability is computed mainly with the aim of dealing with the apparent absence of DNe in GC, we do not have any prescription for P_{obs} associated with CVs having stable discs. Thus, equation (8) is associated with DNe only.

3.5 Additional considerations

So far, we have described the main aspects of the CATUABA code used to study the PDP of CVs present in GCs simulated by MOCCA. None the less, other options are available in the code that allow for studying aspects of the CVs not only included in the PDP. Now, we turn to such options.

3.5.1 Destroyed CVs

Throughout the evolution of a GC in the MOCCA code, not only are the CVs in the PDP formed, but many other CVs are formed as well. The only difference is that they do not survive up to the present day. One of the capabilities of the CATUABA code is the ability to collect relevant information about such systems, in order to investigate their properties and the reasons for their absence in the PDP.

This option gives similar information as given by the study of the PDP. The main difference is that the information regarding the PDP is replaced by the information associated with the destruction-age population which correspond to the CV properties immediately before their disappearance from the cluster.

With such a sample, one can investigate the properties of such 'destroyed'[4] CVs and also delineate general destruction channels.

In the possession of such information, we can separate the CVs into groups, according to the main channels of 'destruction' (similarly to what is done for the CVs in the PDP). Our choice on the matter is as follows. (i) *Destruction due to binary stellar evolution group*: the CV stops being a CV due to some evolutionary process and *without* any influence from dynamical interactions. (ii) *Destruction due to escape*: the CV life in the cluster is interrupted because the CV escaped the cluster while still being (or not) a CV after the escape. (iii) *Destruction due to dynamical interaction group*: the death of the CV was caused by a dynamical interaction, but the outcome of this interaction remains in the cluster.

Notice that a CV can escape from the system due to either relaxation processes or dynamical interactions. Both cases here are related to the destruction due to escape group. In the case associated with CVs destroyed by dynamical interactions without escaping, such CVs belong to the destruction due to dynamical interaction group.

3.5.2 Field-like CVs

Two other important tools in the code are the possibility to run the BSE code alone for the initial binaries and for the escaping binaries. The former allows one to study the field-like population (without dynamics) of CVs that comes from the initial binaries. This permits one to investigate how different the cluster and field-like populations are, or even constrain the initial distributions of binaries with available data from observed CVs in the solar neighbourhood. The latter allows the study of the escaping CV evolution and the evolution of escaping binaries that will become CVs up to 12 Gyr.

Again, for the BSE runs, similar information is recorded about progenitor population, formation-age population, PDP and destruction-age population. In the case when BSE evolves the initial binaries, information about the progenitor population, formation-age population and PDP is saved for the CVs that survive up to 12 Gyr. If the CV is somehow 'destroyed', then the information about the destruction-age population is saved instead of the information about the PDP. When BSE is run for the escaping binaries, additional information is saved for the binaries immediately after the escape. This would correspond to the escaping-age population. Again, information about the formation-age population is saved always and, about destruction-age population or PDP, whether or not the CV survives up to 12 Gyr.

3.5.3 Time dependence of CV properties

The last resource provided by the CATUABA code in its current version is the possibility to investigate the time-dependent properties of the CVs from the cluster birth up to the present day. Such an option in the code utilizes the cluster snapshots. For a particular snapshot, all CVs present in it are collected and their semi-major axis, period,

[3] The quantity t_{dur}/t_{rec} corresponds to the very DN duty cycle.

[4] The reader should keep in mind that the term 'destroyed' used here is not necessarily associated with a destructive process *stricto sensu*. The term adopted here has a more general sense: CVs that are created during the cluster evolution but do not survive up to the present day due to many reasons.

mass ratio and mass distributions are generated. This is done for all the snapshots of the cluster (every 200–250 Myr, depending on the cluster). It provides an efficient way to investigate how such distributions evolve with time. Apart from the distributions, the code also saves the average and median values of the semi-major axis, period, mass ratio and masses through time, again, based on all snapshots.

This option is available for the MOCCA snapshots and also for the BSE snapshots, when one is interested in comparing both populations of CVs. In this case, the timesteps for generating the snapshots of the cluster in MOCCA and BSE have to be the same. In the case when only BSE snapshots are being analysed, the timestep for the creation of such snapshots can be any value. The timestep associated with MOCCA snapshots is defined before the simulation, and this value has to be used in the CATUABA code.

Here, we summarize all the possible ways of using the CATUABA code as described above.

3.6 Summary of CATUABA features

In order to account for the limitations of the above-presented approach, we present a summary it and address the principal hypothesis which should be kept in mind when interpreting the results presented in this series of papers (especially, in Section 5.5 of this paper). The study of the CVs is carried out in the following way.

(i) The first step is to recognize the PDP of the CVs in the snapshot of the cluster at 12 Gyr. The next is to compile the most relevant events in the history of all the stars in the PDP. With this, we can unequivocally separate the CVs into three groups, namely BSE group, WDI group and SDI group.

(ii) The second step is to cover the shortcomings for CVs with stable or unstable discs. This is done by considering the formalism in the DIM. Such *modus operandi* provides good agreement with observation, and also allows for filling the deficiencies left by BSE.

(iii) The third step is to compute two important time-scales of DNe, namely recurrence time and duration of the outburst. This is done by using empirical relations.

(iv) The fourth step is to calculate the probability of observing and detecting the DNe by means of equation (8).

It is rather important to mention at this point that we do not have any prescription for magnetic CVs. They correspond to roughly 25 per cent of CVs in the field (e.g. Wickramasinghe & Ferrario 2000; Ferrario, de Martino & Gänsicke 2015) and can be extremely important in GCs (e.g. Grindlay et al. 1995; Dobrotka et al. 2006; Ivanova et al. 2006).

Secondly, most short-period DNe are SU UMa stars which also have superoutbursts in addition to normal outbursts. Superoutbursts are more luminous (increase in brightness by ∼1 mag), last longer (10–20 d), and are more infrequent (every 3–10 DN cycles). In this way, the chances to observe a short-period DN during superoutburst are even smaller since for one superoutburst, we have 3–10 outbursts. Since we are interested here in the upper limit of the probability, we neglect this complication.

Thirdly, the values for the accretion rate and, in turn, luminosities and magnitudes, are derived based on maximum values provided by the DIM. Besides, the mass transfer rate computed is a rough estimate since it is based on average value of the donor mass-loss during the CV evolution.

Finally, all information obtained in the CATUABA code is associated with the BSE code. Thus, it is limited by what the BSE code is capable of.

To sum up, the principal hypothesis developed in this work includes the neglect of magnetic CVs and superoutbursts for the short-period DNe; the extrapolation of empirical relations for the CVs; the assumption of theoretical maximum values for the accretion rate, and consecutively, maximum luminosities. All these assumptions have the aim of computing the upper limit for observing the CVs.

It is worth noticing that the procedure described above is somewhat forged, although reasonable. This is because we cannot retrieve precisely the CV properties from observations.

Other options can be used independently from what is done for the CVs in the PDP (Section 3.5). A flow chart of the code is presented in Fig. 1. In the very beginning, the user has to choose an option which includes

(i) getting the PDP, the progenitor population, the formation-age population and the observational properties for the CVs present in the cluster at 12 Gyr;

(ii) getting the progenitor population, escaping-age population, formation-age population and destruction-age population for the CVs formed during the cluster evolution but not present in the PDP;

(iii) getting the progenitor population, formation-age population and destruction-age population/PDP for the field-like CVs;

(iv) getting the progenitor population, formation-age population and destruction-age population/PDP for the CVs created from escaping binaries;

(v) getting the distributions of the main orbital elements of the CVs though time.

Notice that this flow chart reflects the underlying coding structure and is not meant to represent a logical flow or progression in the data analysis.

After introducing the CATUABA code and also the hypothesis in it, we are able to turn to the description of the six models (Section 4) that are used in these initial investigations and the main results on the PDP of CVs in such models (Section 5).

4 MODELS

In this first examination of CVs in GCs, we have chosen six models that differ mainly with respect to the initial central density, initial binary distributions and initial binary fraction. The restricted number of models used in this work is due to its very objective nature: to construct the numerical apparatus used to study CVs based on MOCCA simulations, to check its consistencies and to gain experience for data analysis.

Before proceeding further, it is convenient to define the initial binary population (IBP) since it is a rather important concept in this work. The initial binaries in GCs follow determined distributions for their parameters: semi-major axis, eccentricity, masses, mass ratio and period. Hereafter, the initial binaries associated with the initial distributions for their parameters belong to the IBP. In other words, the IBP is the group that contains all initial binaries, in a given initial cluster, associated with specific initial distributions for their parameters. In this work, we analyse models with two distinct IBPs.

The first set of models, defined as the K models, corresponds to models constructed based on the IBP derived by Kroupa (1995, 2008) and Kroupa et al. (2013). Such an IBP has the following properties: (i) the period distribution favours long-period binaries; (ii) the orbits tend to be circularized for short-period binaries, and (iii) the mass ratio distribution is almost flat with a huge peak close to ∼1.0 (Marks, Kroupa & Oh 2011). The K models have 95 per cent

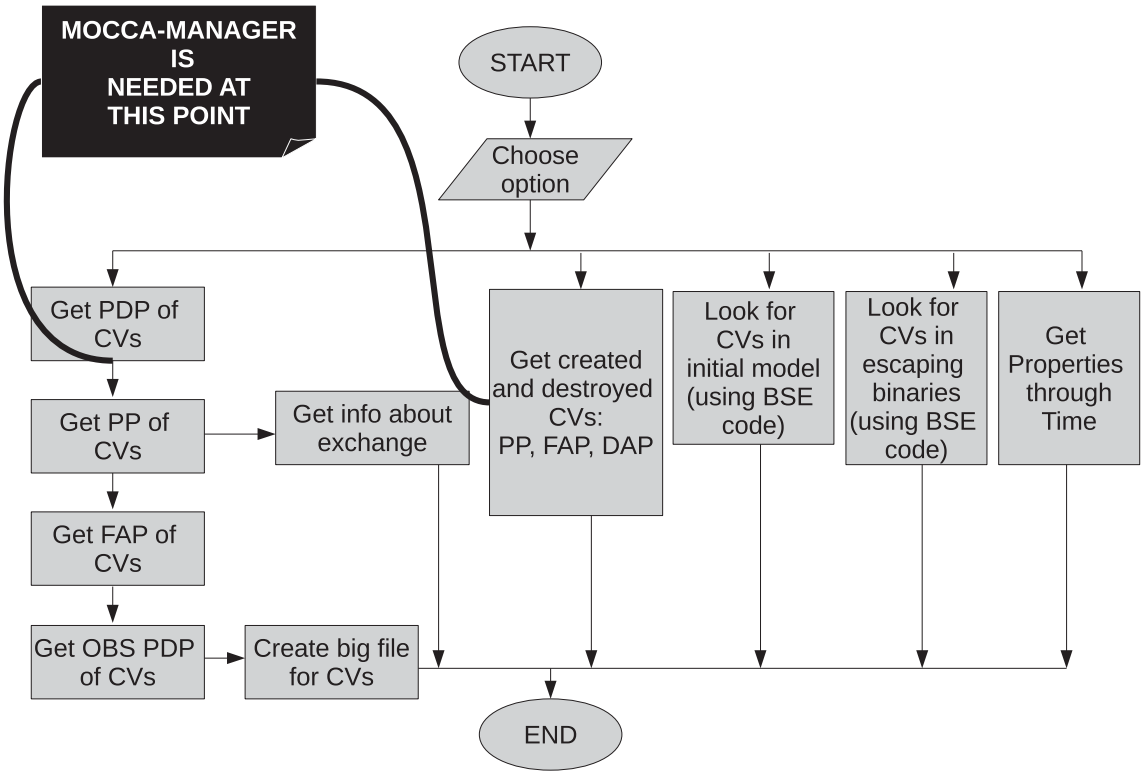

Figure 1. Flow chart of the CATUABA code. Notice that to get the info about progenitor population and formation-age population, for CVs present (or not) in the cluster at 12 Gyr, the files containing the very detailed history of the stars lives are needed. This is obtained by using the MOCCA-MANAGER code. Notice that this flow chart reflects the underlying coding structure and is not meant to represent a logical flow or progression in the data analysis.

primordial binaries,[5] the same initial mass $8.07 \times 10^5\,M_\odot$ and the same initial number of objects (binaries and single stars) 1.12×10^6. But they differ with respect to the initial central density, having, in $M_\odot\,pc^{-3}$, 1.9×10^2, 7.8×10^4 and 3.2×10^5. Thus, we have one sparse model, one dense model and one very dense model.

The other set of models, defined as S models, follows the 'Standard' IBP and has low binary fractions of 5 and 10 per cent. The Standard IBP is associated with a uniform distribution for the mass ratio, a uniform log or lognormal distribution for the semi-major axis and a thermal distribution for the eccentricity. As in the K models, we have chosen models with different initial central densities, namely 2.8×10^3, 1.3×10^5 and 5.9×10^5, in $M_\odot\,pc^{-3}$. Again, for the set of S models, we have a sparse model, a dense model and a very dense model. Differently from the K models, in the S models, we have different initial numbers of objects and initial masses.

We have used two IMFs that follow the broken power law $\xi(m) \propto m^{-\alpha}$, defined by Kroupa et al. (1991, 1993). The IMF2 (canonical) is such that it has $\alpha = 1.3$ for $0.08 \leq m/M_\odot \leq 0.5$ and $\alpha = 2.3$ for $0.5 \leq m/M_\odot \leq m_{\rm max}/M_\odot$ (Kroupa 2008). The IMF3 (multiple power law) is such that it has $\alpha = 1.3$ for $0.08 \leq m/M_\odot \leq 0.5$, $\alpha = 2.3$ for $0.5 \leq m/M_\odot \leq 1.0$ and $\alpha = 2.7$ for $1.0 \leq m/M_\odot \leq m_{\rm max}/M_\odot$ (Kroupa 2008). The star mass in this study lies between 0.08 and 100 $M_\odot$.

We assume that all stars are on the zero-age main sequence when the simulation begins and that any residual gas from the star formation process has already been removed from the cluster. Additionally, all models have low metallicity, are initially at virial equilibrium and have neither rotation nor mass segregation. Moreover, all models are evolved for 12 Gyr which is associated with the present day in this investigation.

In Table 1, we summarize the main parameters of the initial models.

In addition to the evolution done using MOCCA, we have also evolved the initial models (actually, the IBP) with BSE alone during 12 Gyr. In such a way, we will have information not only about the cluster CVs but also on the field-like CVs. This will help us to compare both groups of CVs that come from the six initial models.

5 RESULTS AND DISCUSSION

In this section, we present the main results related to the PDP of CVs in the six models described in Section 4. First, we will discuss some evolutionary properties of the models. Secondly, we will state the properties of the PDP of CVs. After that, we will show how observational selection effects can hide the CV population in observed GCs by computing the upper limit of observing such CVs. We also address some discussions on the main points and correlate this work with previous ones. Finally, we discuss possible observational procedures that might help in detecting the missing DN population.

5.1 Cluster evolution

The clusters were evolved to an age of roughly 12 Gyr – considered here as the present day – which required one day in the PSK cluster at the Nicolaus Copernicus Astronomical Centre (CAMK) in Poland.

[5] We set the initial binary fraction for the models with Kroupa IBP different from 100 per cent in order to avoid computational problems that arise in MOCCA if there is no single star in the initial model.

Table 1. Models and parameters that define them. The name of each model has a letter and a number. The letter indicates its IBP as well as its initial binary fraction, namely K (Kroupa) with high initial binary fraction and S (Standard) with low initial binary fraction (see the text); and the number indicates its central density: 1 (sparse), 2 (dense) and 3 (very dense).

Model	Mass ($M_\odot$)	Number of objects	Initial binary fraction %	Central density ($M_\odot$ pc^{-3})	r_t (pc)	r_h (pc)	Z	IMF[a]	q[b,c]	a[b,c]	e[b,c]	Present-day type[d]	Present-day binary fraction %
K1	8.07×10^5	1.12×10^6	95	1.9×10^2	115	16.9	0.001	3	Kroupa	Kroupa	Kroupa	pc	28.3
K2	8.07×10^5	1.12×10^6	95	7.8×10^4	115	2.3	0.001	3	Kroupa	Kroupa	Kroupa	cIMBH	8.9
K3	8.07×10^5	1.12×10^6	95	3.2×10^5	72	1.4	0.001	3	Kroupa	Kroupa	Kroupa	cIMBH	5.4
S1	5.92×10^5	1.00×10^6	05	2.8×10^3	97	7.5	0.000 16	3	Uniform	Lognormal	Thermal	c	4.9
S2	9.15×10^5	1.80×10^6	10	1.3×10^5	125	2.1	0.001	2	Uniform	Uniform in log (a)	Thermal	pc	4.8
S3	1.52×10^5	3.00×10^5	10	5.9×10^5	69	0.7	0.001	2	Uniform	Uniform in log (a)	Thermal	c	4.6

[a]The IMF3 is the Kroupa IMF with three segments (Kroupa, Tout & Gilmore 1993) and the IMF2 is the Kroupa IMF with two segments (Kroupa, Gilmore & Tout 1991).
[b]The Kroupa IBP corresponds to the construction of the parameters based on the eigenevolution and the mass feeding algorithm (Kroupa 2008).
[c]The Standard IBP is associated with uniform distribution for the mass ratio, uniform distribution in log or lognormal one for the semi-major axis and the eccentricity thermal distribution is such that it follows from a uniform binding-energy distribution.
[d]The cluster present-day type can be post-core collapse (c), post-core collapse with intermediate-mass black hole (cIMBH) and pre-core collapse (pc).

The last two columns of Table 1 show the properties of the clusters at the present day. Notice that for six models, we have relatively representative models, including sparse, dense and very dense clusters; high and small initial binary fraction; post-core collapse clusters and two with intermediate-mass black holes.

Also important is that the binary fraction in models K1, K2 and K3 drops drastically in the early evolution of the clusters, since the soft binaries tend to be disrupted. This is due to the interplay between the cluster densities and the initial distribution of the period in the Kroupa IBP which is dominated by soft binaries. Besides, the denser the cluster, the faster the decrease in the number of binaries (see the last column of Table 1).

Previous studies on CV and also on AM CVn (interacting binary in which a WD accretes matter from another WD) were performed on the basis of the Standard IBP (see Section 4). This is the first work which includes not only such Standard IBP but also the Kroupa IBP. Interesting results come from the Kroupa IBP (e.g. Kroupa 1995, 2008) which can reproduce, to some extent, some observable properties of the binaries in the Galactic field. Nevertheless, the Kroupa IBP was never tested with respect to the observed CV properties. In this way, analysing such models will allow for the first time checking the consistency of the Kroupa IBP regarding CVs, especially those in the field since most stars in the field should have come from the dissolution of star clusters (e.g. Lada & Lada 2003).

5.2 Dependence on initial model

We can start the analysis of the PDP of CVs by providing the number of CVs in each model separated by the three groups described in Section 3.2. This is given in Table 2. We also included in the table the CVs formed due to exchange. In addition, we include the number of binaries in the progenitor population that become CVs when BSE is run alone, i.e. binaries that would become CVs no matter the number/strength of dynamical interactions, if any took place. Finally, in the last column of the table, we state the number of CVs formed when evolving the IBP out of the cluster evolution, i.e. evolving all the initial binaries with the BSE code alone. This is the field-like population of CVs that comes from the respective IBP.

Table 2. Number of CVs that are present in the clusters at 12 Gyr separated by the group to which they belong, namely binary stellar evolution (BSE) group, weak dynamical interaction (WDI) group or strong dynamical interaction (SDI) group. Also indicated is the number of CVs for which exchange is the main channel for their formation as well as the number of progenitors of the CVs (binaries in the progenitor population) that become CV when BSE code is run alone, i.e. that become CVs purely via binary evolution without the cluster environment. The last column indicates the number of CVs obtained when BSE evolves all the initial binaries and correspond to the number of field-like CVs that come from the respective IBP.

Model	BSE[a]	WDI[b]	SDI[c]	Total	Exchange	CVF[d]	Field-like[e]
K1	0	0	3	3	2	0	0
K2	0	18	164	182	120	0	0
K3	0	9	121	130	98	0	0
S1	40	1	1	42	1	41	69
S2	116	113	31	260	13	197	239
S3	9	14	4	27	2	21	64

[a]CVs that are formed due to binary stellar evolution only.
[b]CVs that are formed with the influence of weak dynamical interaction.
[c]CVs that are formed with the influence of strong dynamical interaction.
[d]CVs formed when BSE code evolves the progenitors of the CVs (binaries in the progenitor population).
[e]CVs formed when BSE code evolves all the initial binaries.

5.2.1 *Absence of field-like CVs in Kroupa models*

It is clear from the table that there is no CV produced via only binary stellar evolution in the model with Kroupa IBP. In other words, in order to form CVs in the models with Kroupa IBP (K1, K2 and K3), dynamical interactions have to take place. This is a strong hint towards an inconsistency between observations and theoretical predictions, because we do observe CVs in the field and regions where dynamics could not have played a role. Either we are missing important physics or the assumption of a Kroupa IBP is not the right one here.

It is thought that the field population of stars comes from the dissolution of star clusters (e.g. Lada & Lada 2003; Marks & Kroupa 2012) after the expulsion of the residual gas in the star formation process. The simulations here were performed such that the initial clusters are set after the removal of such residual gas. Thus, if the cluster is quickly dissolved due to mass removal because of supernovae and stellar evolution of the most massive stars, the

binary parameters would not be strongly modified (particularly the short-period ones that could be progenitors of CVs). So such a population that comes from the dissolved clusters should represent the field population. In other words, dissolved clusters associated with Kroupa IBP should correspond to the field parent population of binaries (Kroupa 1995). Hence, since they have around 10^6 initial binaries, we should expect a reasonable number of CVs formed from them due to stellar binary evolution only.

Surprisingly, not a single CV was produced in models K1, K2 and K3, even when evolving the IBP with BSE alone. The reason could be either the mass feeding algorithm that increases the mass ratio of the binaries that would be potential progenitors of the CVs might require adjustments or the efficiency of the CEP should be much smaller.

With respect to the mass feeding, the mass ratio associated with the progenitor binaries of CVs is small ($q \lesssim 0.2$) and they are short-period binaries. Since the mass feeding procedure tends to increase the secondary mass due to accretion of gas from the circumbinary material, the secondary mass increases while the primary mass remains constant (Kroupa 2008). This implies that the initial mass ratio of short-period binaries increases towards 1. In this way, it seems that the feeding procedure generates initial binaries that are inappropriate for evolving into CVs, independently of their orbital period distributions.

On the other hand, this difficulty would be overcome if the CEP efficiency decreases significantly. Then a great deal of orbital energy would be needed in order to eject the common envelope; this would bring the long-period binaries (with low q) to shorter periods, and consecutively turn them into potential CVs. Currently, the adopted value is $\alpha = 3.0$. By reducing this value to $\lesssim$1.0, some CVs could be formed.

The Kroupa IBP has been checked against numerical simulation and observations, and has successfully explained observational features of young clusters, associations, the Galactic field and even binaries in old GCs (e.g. Kroupa 2011; Marks & Kroupa 2012; Leigh et al. 2015, and references therein). Nevertheless, our results show that the Kroupa IBP cannot form CVs without the influence of dynamical interactions, given the adopted parameters in BSE.

We will leave for a separate paper a more elaborate discussion on the Kroupa IBP and the stellar binary parameters.

5.2.2 *Influence of dynamics*

Yet with respect to Table 1, we see from the last two columns how dynamics are important regarding CVs in GCs. Since these columns represent the number of CVs formed without the influence of dynamics and survive up to the present day, we can see somehow the influence of dynamics in the S models.

For model S1, almost all CVs are formed from primordial binaries (compare the fifth and seventh columns). This is because this model is sparse. Additionally, we see that some CVs that are formed in a field-like environment are missing in the cluster (compare the seventh and last columns). This indicates that dynamics in such a cluster contribute to lower the number of CVs produced in the cluster environment by destroying either their progenitors or the CVs themselves.

For models S2 and S3, we see that not all CVs in the PDP come from primordial binaries (compare the fifth and seventh columns). This indicates that some CVs were formed dynamically. Besides, some CVs or some of their progenitors are destroyed in the cluster environment (compare seventh and last columns) like in model S1. Thus, dynamics in models S2 and S3 contribute to both the creation and destruction of CVs.

For models K1, K2 and K3, we have formation only with the influence of dynamical interactions. Specifically, exchange being the most important channel for the formation of CVs in these clusters, which happen for 2/3 of the entire PDP of CVs. Then, for the sparse cluster K1, the 'dynamical' process of formation is not expressive and only three CVs could form in such a cluster. However, for the denser clusters (K2 and K3) in the set, this is not true. They have a reasonable number of CVs formed because of dynamical interactions since such interactions took place more frequently in K2 and K3 than in K1.

Unfortunately, more details about how the initial density and IBPs influence the CV formation are not obtained by only analysing the PDP of CVs in each model. In fact, we need information about the production/destruction of CVs through the cluster evolution as a whole, i.e. the complete formation rate of CVs in the models.

5.3 CV properties

Now, with respect to the CV properties themselves, in Fig. 2, the WD and donor masses of the CVs at the present day are displayed. We also included in the figure (last panel) the PDP of all six models aggregated as one.

5.3.1 *WD mass*

We can see clearly a distinction between CVs strongly influenced by dynamics and CVs which were not strongly influenced. The former has a peak around 0.7 $M_\odot$ while the last has a peak around 0.3 $M_\odot$ for the WD mass. Additionally, the former belong to the SDI group while the latter to the BSE group. In this way, dynamics bring more massive accretors to the PDP. This is because of the exchanges that take place in the CVs belonging to the SDI group. In this case, it is more probable to exchange a low-mass star for a more massive star in dynamical interactions. Thus, the future accretor will be more massive.

Concerning the WDI group, if the cumulative effect of the weak interactions in the binary that becomes CV is strong, then such a CV will have properties similar to those in the SDI group, as in the case of the CVs in models K2 and K3. On the other hand, if the net effect of the weak interactions is soft, then the CV will have similar properties as those of the BSE group. This can be seen in models S2 and S3.

Generally, with respect to all analysed models, each CV in the WDI group suffered few weak dynamical interactions before the CV formation. Around 37 per cent of the CVs in the WDI group suffered only one dynamical interaction, ∼20 per cent suffered two and ∼10 per cent suffered three weak interactions. The rest of them suffered more than three weak interactions. Surprisingly, there is one CV that went through 28 weak dynamical interactions. Now, after the CV formation, most of them suffered only one weak dynamical interaction which changes slightly the eccentricity by an amount of $\sim 10^{-8}$.

Concerning the CVs (in all six models) in the SDI group, they suffered few strong dynamical interactions before CV formation. Most of them (∼71 per cent) experienced only one strong dynamical interaction. Around 20 per cent underwent two strong dynamical interactions and ∼6 per cent of them went through three strong dynamical interactions. The rest of them (∼3 per cent) suffered four or more strong dynamical interactions. There is one CV that went

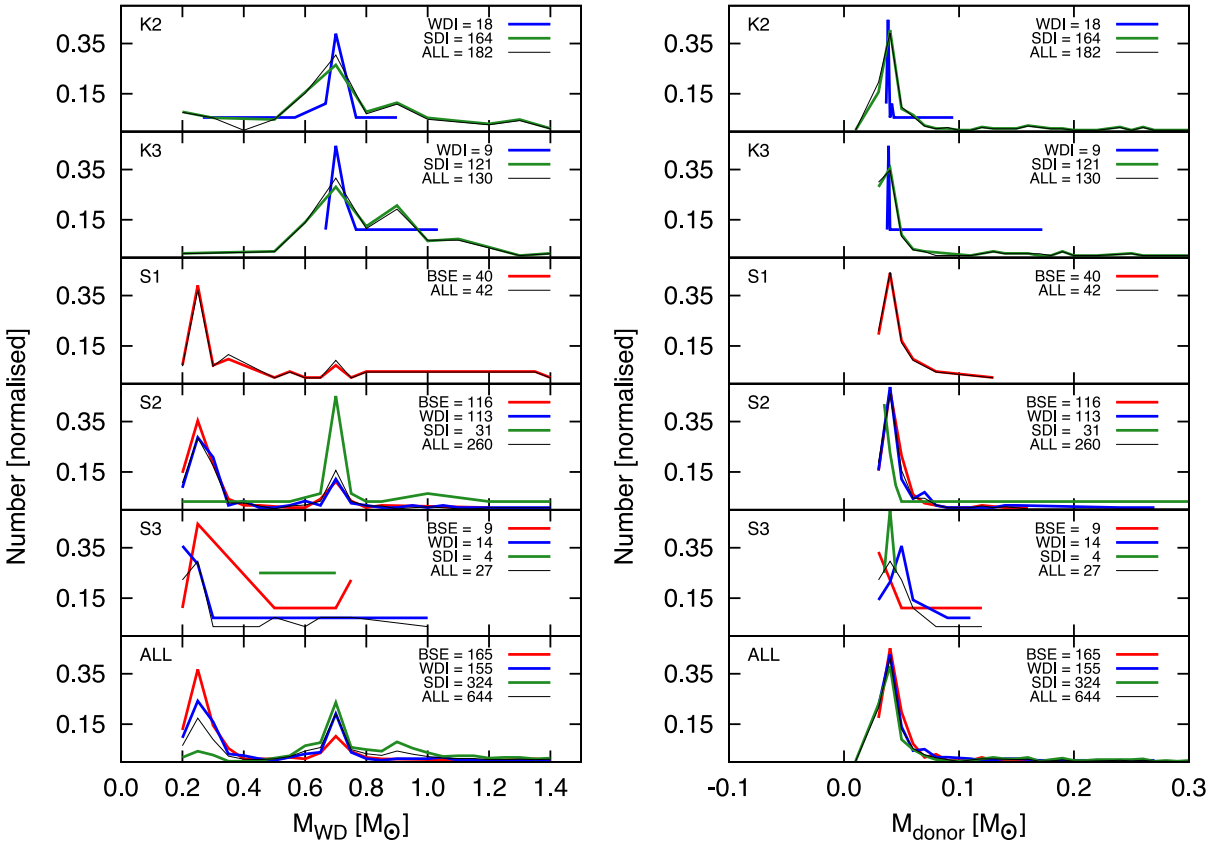

Figure 2. Present-day CV component masses, normalized by the total number indicated in the key. Left: the WD mass with distinction for the groups of CVs, namely BSE, WDI and SDI. Notice that the CVs in the SDI group have masses peaking around 0.7 $M_{\odot}$ and the BSE group contains CVs whose WD mass is peaked around 0.3 $M_{\odot}$. Right: the donor mass. Notice that for the donor, we do not observe any difference associated with the influence of dynamics, i.e. the three groups have very low mass donors, in general. The keys indicate the number of CVs in each model and group, and the last panel represents the PDP of CVs present in all six models aggregated as one.

through seven strong dynamical interactions before CV formation. Regarding the evolution after CV formation, only one CV in one model went through one strong dynamical interaction.

5.3.2 Donor mass, period and CV status

In Fig. 2, we see no difference among these groups with respect to the donor mass. The majority of the CVs in the six models have BD companions. This means that they are mainly in the last stage of CV evolution (∼87 per cent are period bouncers with BD as donor). The reason for that is simple, the CVs are formed mainly in the domain of short-period CVs which means that they will easily evolve up to the period bouncers domain.

Obviously, not all CVs in the PDP are period bouncers. The youngest CVs are still short-period CVs, long-period CVs or CVs in the gap. Nevertheless, considering 12 Gyr of cluster evolution, it is reasonable to have most of them as period bouncers. This has already been shown by Howell et al. (1997), for instance, for CVs in the Galaxy.

Apart from the masses of the stars in a CV, the period has come out to be one of the most important observables on the matter. For the PDP of CVs in the six models, we do not observe the period gap (most of the CVs are formed below or in the gap) and the period distributions peak around 3 h (in the period bouncers domain).

At this point, we can state the main characteristic of the PDP of CVs in GC: they are in (or close to) the last stage of their evolution, as one can see from Fig. 2. This not only defines their properties but also indicates that observational selection effects can be rather strong and have to be taken into account for a consequential understanding of CVs in GCs (e.g. Pretorius, Knigge & Kolb 2007; Knigge 2012).

After a brief discussion on the CV properties, we can concentrate on the observational selection effects associated with the PDP of CVs in the six models which, in turn, is totally bound to the PDP thereof.

5.4 Are CVs in GCs DNe?

One of the objectives of this work on CVs and related objects is to quantify the influence of observational selection effects on the analysis and prediction done by models. In this sense, we decided to implement in the CATUABA code an upper limit for the probability of detecting CVs as a function of distance and limiting magnitude. This choice was motivated by the aim of showing that, if we find small chances to detect CVs, even in a perfect situation, then, in real situations, it will be worse. This seems to be an extremely important topic and should be associated with the so-called absence of DNe in GCs.

The first step in the direction of computing the fraction of CVs expected to be observed during an ideal night with an ideal instrument is checking if the CVs in the PDP are DNe or not. Using equations (1) and (2), we can separate the CVs into three ranges with

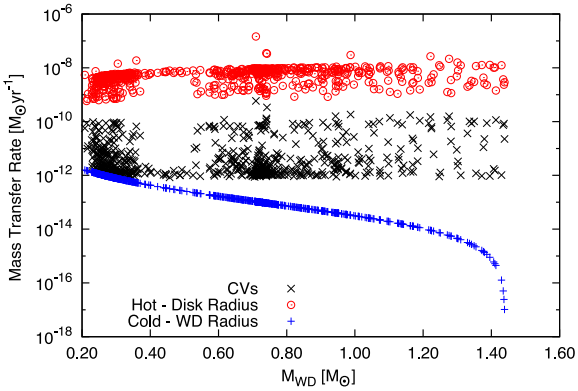

Figure 3. Comparison of the values of the mass transfer rate required for a full CV disc to be globally hot and stable (circles) or globally cold and stable (plus signs) with respect to the mass transfer rate of CVs in the PDP (crosses). One can notice that all CVs are DNe and the mass transfer rates of the CVs are such that it allows for the instability somewhere in the disc. It is also possible to realize that the instability for many CVs takes place very close to the inner edge (crosses close to the plus signs).

respect to the disc stability as described in Section 3.3.1. Fig. 3 shows that all CVs in the six models are potential DNe. Additionally, the figure illustrates clearly that for a great deal of them, the instability takes place quite close to the WD surface (crosses close to field plus signs). This indicates that the strength of the WD magnetic field does not have to be very strong in order to prevent the disc instability and, in turn, the outbursts in such systems. Fortunately, this is not bad for our purposes since we are trying to derive an upper limit for the real probability of detecting the CVs. In this way, having a disrupted disc (cold and stable) would lower the probability even further.

Once we know that the CVs are DNe, we are able to compute the recurrence time and the duration of the outburst, based on equations (6) and (7). The results are displayed in Fig. 4. Notice that the recurrence time varies from days to decades and the outbursts last a few days. Notice also a double peak in the distribution of the recurrence time due to the double peak in the WD mass. Dynamically formed CVs have greater WD masses, implying longer recurrence times according to equation (6). Now, for the distribution of the duration of the outburst, we do not see too many differences between dynamically formed CVs and CVs formed without influence of dynamics. This is due to the status of the CVs at the present day (period bouncers). They mainly have periods from ∼2 to ∼3 h and according to equation (7) (which is a function of the orbital period) they are similar.

From Fig. 4, we can see that the chances to observe a CV during outburst are high only for some CVs – the youngest ones that were formed close to the present day and have greater donor masses and higher mass transfer rates with respect to the old ones. In this way, we have the first clue that a good solution would, instead of looking

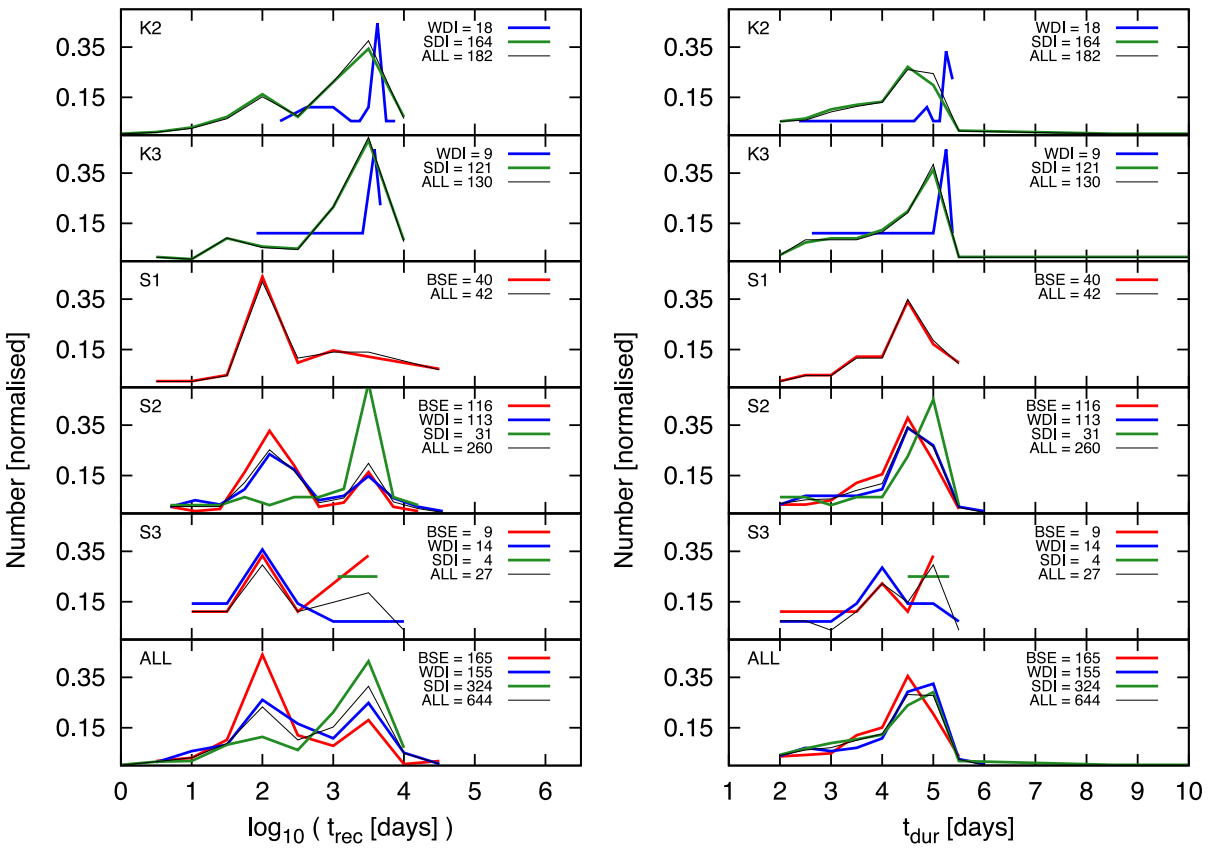

Figure 4. Recurrence and duration times associated with the DNe CVs present in the PDP. Notice that the outbursts last a few days and the intervals between them are from a few days to decades. Notice a double peak in the recurrence time distribution due to the double peak in the WD mass distribution. Dynamically formed CVs have greater WD masses, then longer recurrence times according to equation (6). Now, for the duration of the outburst distribution, we do not see too great of differences between dynamically formed CVs and CVs formed without influence of dynamics. This is due to the CV status at the present day (period bouncers). Most of them have periods from ∼2 to ∼3 h, and according to equation (7) (which is a function of the orbital period), they are similar.

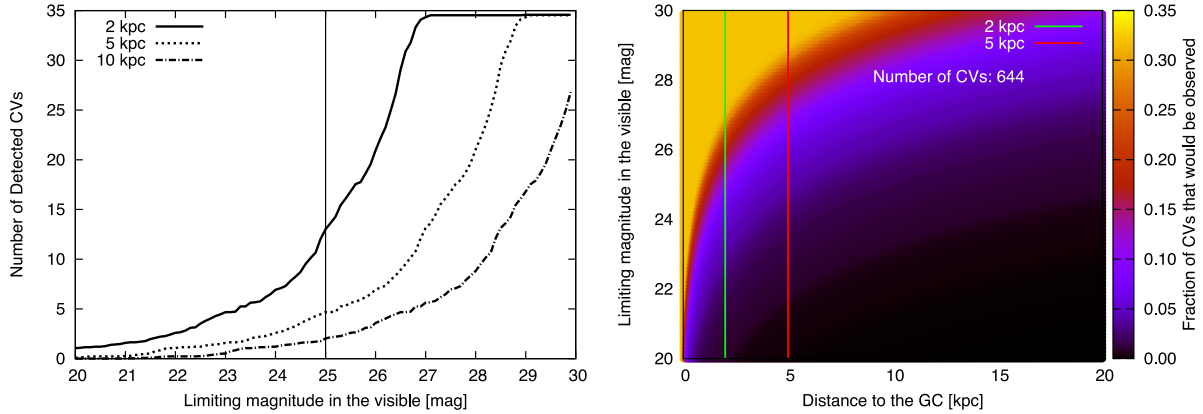

Figure 5. Left-hand panel: number of CVs that could be observed in an average GC as a function of the limiting magnitude for three different cluster distances. Right-hand panel: CV detection rate as a function of the limiting magnitude and the cluster distance, considering all CVs in the six models. The colour bar represents the CV fraction that would be observed based on probability-weighted 2D normalized histograms in each cell of size 0.005 × 0.1.

for variability during an outburst, look for it during quiescence. The biggest problem associated with this approach is the need of very deep observations because in order to reach magnitudes similar to those associated with a CV during quiescence, one needs deeper observations in comparison with the same CV during its outbursts. Although a difficult task, it is possible. For instance, Cohn et al. (2010) reached apparent visual magnitudes as deep as ∼26 when studying the optical counterparts of X-ray sources in the GC NGC 6397.

5.5 Probability of detection through variability

Now, once we have separated the CVs with respect to the disc instability and computed their recurrence times as well as the duration of their outbursts, we can turn to the computation of the probability of detecting such CVs by using equation (8).

The left-hand panel of Fig. 5 displays the number of CVs that would be observed as a function of the limiting magnitude for three different cluster distances, considering the PDPs in all six models (644 CVs). Thus, the number of CVs indicated in the figure is related to the number of CVs that would be observed in an 'average' GC since it is associated with the total number of CVs seen in all models divided by the number of clusters (i.e. six). In this average cluster, the total number of CVs is ∼108. For instance, for a limiting magnitude of 25 mag, at 2 kpc, one would observe ∼13 CVs. For 5 and 10 kpc, one would observe ∼5 and ∼2, respectively. As the limiting magnitude increases, the number of observed CVs increases up to a maximum of ∼1/3 (fraction of eclipsing CVs).

The right-hand panel of Fig. 5 is a generalization of the left-hand panel and exhibits the CV fractions that would be detected weighted by the probability of observing each CV in each cell of size 0.005 × 0.1, computed based on normalized histograms in the plane of limiting magnitude versus distance, including all CVs in the PDP of all six models. Notice that we have basically three regions in the figure: one dark, one light and one in the middle. The dark region corresponds to CVs that could be observed only during outburst since the probability is small. The light region is associated with the CVs that can be observed also during quiescence, because the probability is ∼1/3 (probability of being eclipsing binary). Finally, the middle region (not so dark nor so light) corresponds to a mix of CVs that can be observed during quiescence and during outburst.

In this way, the smaller the distance and the greater the limiting magnitude of the instrument, the greater the chances are to detect the CV during quiescence.

Now we can compare this result with observations and check its consistency. First, if one fixes the position of the cluster, let us say at 2 kpc (corresponding to the distance of the closest GCs and indicated in the figure), and goes from lower limiting magnitudes up to higher limiting magnitudes, we see that the probability is small ($\lesssim$10 per cent), up to about ∼25 mag. Then, from that point up to ∼26.6 mag, the probability increases to ∼20 per cent. From there, the probability reaches the maximum (∼1/3).

As an example for comparison, Cohn et al. (2010, see their fig. 3) reached a limiting magnitude of around 26 mag in the *R* filter (similar filter to what we have) in their observations of NGC 6397. In such a study, they found 15 candidates of CVs. In this way, since the predicted number of CVs in our 'average' cluster is around 100, and our fraction of detectable CVs for such a limiting magnitude is around 20 per cent, we should expect that they would have found around 20 CVs in their search, which corresponds to an upper limit. This conclusion comes from the fact that we are considering an ideal model for the probability of detecting CVs through their variabilities, i.e. Fig. 5 shows the number/fraction of predicted CVs that should be detected in an ideal observation, which does not account for the realities of collecting observational data (e.g. distance, reddening, etc.).

In practice, some effects not considered here would lower the fraction of CVs observed even further, such as

(i) GC are crowded fields;
(ii) large observational errors for faint stars;
(iii) WDs can have magnetic fields strong enough to avoid the instability in the disc (25 per cent, in the field);
(iv) the mass transfer rate computed here is a rough estimation. Thus, some CVs could have smaller mass transfer rates and be inactive instead of being DNe ones;
(v) the number of nights used to observe a specific cluster is less than the entire DN cycle;
(vi) heterogeneous observations unevenly distributed over time;
(vii) the estimate of luminosities is the highest possible in the DIM;
(viii) only normal outbursts are considered. Superoutbursts are present in short-period CVs as SU UMA and are more luminous,

however the recurrence time is much longer; this, in turn, would decrease the probability.

Thus, after including all these complications, one should have only a small fraction of the CVs in a GC detected during the observations for a relatively low limiting magnitude such as ∼26 mag. At least half of the predicted number would be expected.

5.6 Future observations

From the last subsection, we realize that, in order to reach good detection rates through variability, one would have to observe the CVs during quiescence in very deep observations ($\gtrsim$27 limiting magnitude) and in not too remote GCs ($\lesssim$5 kpc). For the typical limiting magnitudes achieved in previous surveys (e.g. Shara et al. 2005; Pietrukowicz et al. 2008) and previous observations (e.g. Cohn et al. 2010), only a very small fraction of the CVs (considering that they are DNe) would be seen. So, it is not surprising that they detected only a small number of CVs.

Fig. 5 is quite instructive and poses quite an interesting result: CVs in GCs are not, a priori, non-DNe. In other words, it is not easy to rule out the notion that most CVs in GCs are DNe, especially by considering observational selection effects. Even though the idea that CVs in GCs are preferentially magnetic has been largely accepted and treated as coherent, from our results we cannot discard the possibility that most of them are DNe, and due to observational selection effects, we are not able to always detect them during (e.g. Servillat et al. 2011; Webb & Servillat 2013).

To sum up, any of the problems mentioned in Section 5.5 would lower the probability even further and, in turn, not change the main conclusion here that observational selection effects do change what one would expect to observe and that the probability of detecting CVs in observations and campaigns is extremely small.

Thus, what sort of observation should be performed in order to observe the predicted CV populations in GCs?

5.6.1 *Variability during quiescence?*

We could conclude in Section 5.4 that, given the typical mass transfer rate of the predicted CVs, they should be DNe, unless the WD magnetic field is strong enough to disrupt the inner part of the disc. Additionally, we showed in Section 5.5 that the chances of detecting a CV during its outburst are usually small, as its intrinsic duty cycle is small.

One alternative that might help here would be the search for variabilities during quiescence. With such an approach, whether a CV is in quiescence or outburst can be overcome. However, reaching the large magnitudes of faint CVs in GCs might be an issue. Nevertheless, the brightest CVs in a faint population should be detected during deep observations. These correspond to the WZ Sge type of CVs.

WZ Sge CVs have very low mass donors (∼0.08 $M_{\odot}$) and their quiescent stages last decades due to the extremely small mass transfer rate. Furthermore, they are believed to be in the transition stage between short-period and period bouncer CVs. Thus, they are the prototype of the period bouncers of which they are more luminous. Therefore, if there are, indeed, a lot of period bouncers in GCs, the WZ Seg should reveal real trends associated with the CV population in GCs.

This idea has already been proposed by Knigge (2012), and seems reasonable based on our results.

5.6.2 *X-rays*

Most of the predicted CVs in our models have X-ray luminosities between $\sim10^{29}$ and $\sim10^{30}$ erg s^{-1}. Although, a 9 per cent fraction have $L_{\rm X} \lesssim 10^{29}$ erg s^{-1}. As we have already pointed out in Section 1.3, little effort was used in order to recognize counterparts of X-ray sources below $\sim10^{32}$ erg s^{-1}. In this way, more effort should be put forth in order to detect sources below $\sim10^{30}$ erg s^{-1} with secure optical counterparts. This might be difficult, although doable.

Over and above, our results are consistent with what Byckling et al. (2010) found for DNe within ∼200 pc in the solar neighbourhood. However, their sample is small and composed of bright X-ray DNe, which makes the comparison difficult. Nevertheless, if the CVs in GCs are predominantly DNe, then we should be able to detect them in X-ray observations below $\sim10^{30}$ erg s^{-1}.

We might say that looking deeper with *Chandra* may help to disentangle the issue about the nature of CVs in GCs. On the one hand, the X-ray counterparts are biased towards high X-ray luminosities which implies an easier detection of magnetic CVs. Thus, deeper observations would lead to the discovery of potential DNe. On the other hand, the long recurrence time associated with CVs in GCs makes the X-ray identification unlikely in the detection of such DNe, since they live most of their lives in a quiescent stage.

5.6.3 *Other methods*

Once the faint X-ray sources are identified, the next step should be to search for secure optical counterparts. In addition, a combination of Hα and FUV imaging with *HST* might provide almost secure CVs, especially the WZ Sge population, since they are brighter than typical period bouncers.

Alternatively, other approaches could help even more, like the usage of quiescent, late and negative superhumps, which are observed in some SU UMa stars. For instance, Olech, Rutkowski & Schwarzenberg-Czerny (2007, see their fig. 7) found high-amplitude (∼0.7 mag) negative superhumps in BF Ara.

In summary, a great deal of deep observations (combining different approaches) might reveal the missing DNe population in GCs, and increase the knowledge about CVs in GCs as a whole. This set of deep observations yet to come might potentially solve the problem concerning the observed lack of CVs in GCs relative to theoretical predictions.

5.7 Spatial distribution

Another important property from an observational point of view is the spatial distribution of the predicted CVs and their properties with respect to their positions inside the cluster.

Considering the six models, only ∼5 per cent of the predicted CVs are located in the core. Interestingly, most CVs are somewhere between the core and the half-mass radii. This is easy to understand by considering either the relaxation process or the effect of dynamical interactions on CV progenitors.

Generally, there are three physical processes which shape the CV spatial distribution, namely relaxation, dynamical interactions and stellar/binary evolution. For simplicity, let us start thinking of the CVs not affected by dynamics. For such cases, the initial mass segregation (connected with the relaxation process) for the most massive CV progenitors brings them close to the core. After the CEP, the CVs might have masses greater or smaller than the average mass in the core. If a CV has mass greater than the average mass in

the core, then such a CV should migrate inwards, into the core. On the other hand, if the CV has mass smaller than the average mass in the core, then the CV should be pushed outwards, away from the core. For less massive CV progenitors, the above-mentioned process should be the same, although slower.

CV progenitors are among the most massive stars; therefore, the probability for dynamical interactions is effectively large, especially close to the core. For the CVs formed under the strong influence of dynamics, they are usually kicked out from the inner parts of the system due to interactions. Then, if the CV progenitor is massive, it will sink to the core. Although it depends strongly on the cluster evolution itself and if there is energy generation in the core by, for instance, subsystems of black holes, intermediate-mass black holes, etc. In the case of large energy generation in the core, the whole system expands (including the CVs), and so we should not expect many CVs close to the core.

In general, the CV spatial distribution is influenced by relaxation, stellar evolution and dynamical interactions, and drawing a general conclusion might be tricky since there are many issues to be considered in the analysis, like core evolution, CV formation channel, CV formation time, CV initial position, among others.

It is worth mentioning that the young (and bright) CVs in our models are more centrally distributed than the older ones, although the spread is large (due to interactions and different cluster properties).

Our results are in good agreement with the spatial distribution inferred by Cohn et al. (2010), particularly with respect to the magnitude of the CVs. Cohn et al. (2010, fig. 3) show a possible transitional path from the bright CVs to the faint CVs. We also reproduce such a feature in our simulations, although we have many more faint CVs in our data with respect to those that they could detect. This is easily understood by considering the observational limitations of their investigation ($\sim$26 mag) and the predominant magnitude of such faint CVs in our simulations ($\lesssim$27).

6 SUMMARY AND CONCLUSIONS

So far, we have exposed in this paper part of the first results obtained from the analysis of six models simulated by MOCCA using the CATUABA code as well as description of the code itself.

The PDPs of CVs in GCs are in the last stage of their evolution! This, maybe, is the leading characteristic of the CVs in GCs. In addition, if the WD magnetic field is irrelevant, they all are DNe.

In order to check if one could 'easily' observe the DNe with typical limiting magnitudes in previous surveys, a simple (and rather ideal) probability law was derived and computed, whose results are displayed in Fig. 5. It shows clearly that observational selection effects are hiding the real population of CVs in GCs. This can also be thought of with respect to the CVs in the field (Pretorius et al. 2007).

In order to observe the population of CVs in GCs, one should be able to perform deeper observations in such a way that the search would be during quiescence. Something that was already noticed by Knigge (2012) and, to some extent, done by Cohn et al. (2010).

Interestingly, some alternatives exist in order to look for CVs during quiescence. For instance, Cohn et al. (2010) used Hα imaging (which allows a search for short-period variability) in combination with optical observations of *Chandra* X-ray sources. Other ways that might help are FUV with *HST* (Knigge et al. 2003) and quiescent negative superhump (Olech et al. 2007).

In any event, we defend here that the CVs in GCs are not necessarily magnetic. The arguments for magnetic CVs seem to be biased in addition to neglecting some other issues, like observational selection effects and incompleteness in surveys.

As has already pointed out by Knigge (2012), the natural solution to this problem is a survey for DNe in GCs that guarantees the detection of at least a few WZ Sge systems.

More about the CV populations like the progenitor population, the formation-age population and also the evolutionary properties will be discussed, as was said before, in a separate work. Additionally, the apparent problem entailed with the Kroupa IBP is also left to another paper since more models will be needed and an attempt to overcome such an inconsistency will be discussed.

Thus, for this paper, the results displayed in Section 5 can be summarized as follows.

(i) GCs with Kroupa IBP have no CVs formed purely via binary stellar evolution, i.e. dynamics have to act in order to produce CVs. The reason can be either the efficiency of the feeding algorithm or the high CEP efficiency adopted in BSE.

(ii) The main mechanism in CV formation for the Kroupa models is exchange ($\sim$2/3), which is not true for other models (Standard models) in which the main mechanism is the binary stellar evolution.

(iii) Almost all CVs in the present-day clusters are formed below the gap. Additionally, most of the CVs at 12 Gyr ($\sim$87 per cent) are period bouncers with BD as donors, having periods between 1.5 and 3 h.

(iv) We obtained, as in previous simulations, a population of CVs with WDs with small masses ($\sim$0.3 $M_\odot$). Moreover, in our case, the massive WDs ($\sim$0.7 $M_\odot$) correspond mainly to CVs formed because of strong dynamical interactions (mainly exchanges), which is in good agreement with previous works (e.g. Ivanova et al. 2006).

(v) All CVs are DNe if there is no strong WD magnetic field such that it can disrupt the inner part of the disc.

(vi) The duration of the outburst varies from 1 to 10 d and the recurrence time (duration of the quiescent phase) varies from 10 to 10 000 d. This implies that the probability of detecting most of the CVs during outburst is extremely low, even considering an ideal situation in which all nights – during the DN cycle – are observed.

(vii) During quiescence, the eclipsing CVs would be detected in a very deep observation (apparent visual magnitude $\gtrsim$27) in a very close cluster ($\lesssim$5 kpc).

(viii) GCs are old objects which implies that the population of CV tends to be older than the observed population in the field. Thus, at the present day (12 Gyr), the population of CVs is dominated by low-mass donors. In other words, the properties of the population of CV change with time through the cluster evolution and this has to be taken into account for meaningful comparisons between observations and predictions.

(ix) In order to solve the problem regarding the nature of CVs in GCs, additional effort should be put into the optical identification of faint *Chandra* X-ray sources ($\lesssim 10^{30}$ erg s^{-1}) and the utilization of other techniques (e. g. Hα and FUV imaging with *HST*, quiescent negative superhumps) combined together with the aim of detecting almost guaranteed DNe, especially because any conclusions drawn from a comparison between the results of our simulations and observations of CVs with small X-ray luminosities should be taken with a grain of salt, since the observational sample can be regarded as something of an upper limit, due to an increased probability of contamination from active binaries, chromospherically active stars, accreting neutron stars and black holes, etc.

(x) The best region inside GCs to search for CVs should be between the core and half-mass radii.

Finally, some comments are needed concerning the Monte Carlo approach and the population synthesis code utilized in this work.

In Section 2.3, we briefly described some comparisons made between MOCCA and NBODY6 that have led to good agreement between the two. Therefore, we think the approach chosen in this work is reasonable and efficient since the MOCCA code is significantly faster than the most advanced version of NBODY6++GPU.

Even then, the main limitation turns out to be related to the binary stellar evolution code. Some limitations with regard to the CV evolution were commented on in Section 2.1, like the absence of expansion of the donor star for long-period CVs and the old scaling for the angular momentum losses above and below the gap. Nevertheless, from a statistical point of view, such improvements should not change the main conclusions drawn in this work.

7 PERSPECTIVES

The first results of this initial investigation on CVs in GCs are very interesting, especially those associated with observational selection effects and the absence of CVs when using Kroupa IBP. CVs are a potentially useful tracer population for constraining primordial binary distributions as we know the physical mechanisms that drive CV formation and evolution. The IBP can be modified and constrained using CVs by reproducing their observed properties in simulation models.

Nevertheless, this work is just the beginning. Since MOCCA is extremely fast in comparison with *N*-body codes, several hundreds of models can be simulated (and are being simulated) in order to develop a statistical basis the for a constraint of the overall population of CVs in GCs, the correlation between their properties and the cluster properties.

Naturally, investigations not only focused on CVs can and should be done. It is also worthwhile to study CV siblings like AM CVn and symbiotic stars.

Future works will concentrate on the extension of the CATUABA code with the aim of also analysing AM CVn and symbiotic stars. After extending this code, the same six models used here will be used in order to check consistencies and coherence in a similar way done in this initial investigation on CVs.

Once the CATUABA code is fully automated and capable of studying CVs, AM CVns and symbiotic stars in GCs simulated by MOCCA, we intend to apply it to the examination of the MOCCA-SURVEY data base that is being created in the PSK cluster at CAMK. We expect that such an approach will represent a powerful tool in the analysis of particular objects in GCs since the cluster parameter space covered by this survey is huge.

To sum up, as was said, this is the first paper of a series that has the aim of contributing to the most important open questions regarding such fascinating objects and GCs.

ACKNOWLEDGEMENTS

We would like to kindly thank Józef Smak, Arkadiusz Olech and Wojtek Pych for useful discussions and suggestions, which made the quality of the paper increase substantially. We would also like to thank the anonymous referee for the numerous comments that improved this work significantly, especially its presentation. DB is in debt to Józef Smak and Arkadiusz Olech for pleasantly explaining many issues associated with the theory concerning cataclysmic variables. DB was supported by the CAPES foundation, Brazilian Ministry of Education through the grant BEX 13514/13-0. MG, AH and AA were supported by Polish Ministry of Science and Higher Education, and by the National Science Centre through the grants DEC-2012/07/B/ST9/04412 and DEC-2011/01/N/ST9/06000. AA would also like to acknowledge support from Polish Ministry of Sciences and Higher Education through the grant DEC-2015/17/N/ST9/02573 and partial support from Nicolaus Copernicus Astronomical Centre's grant for young researchers.

REFERENCES

Askar A., Szkudlarek M., Gondek-Rosinska D., Giersz M., Bulik T., 2016, preprint (arXiv:1608.02520)
Bassa C. et al., 2004, ApJ, 609, 755
Belczynski K., Kalogera V., Bulik T., 2002, ApJ, 572, 407
Belczyński K., Kalogera V., Rasio F. A., Taam R. E., Zezas A., Bulik T., Maccarone T. J., Ivanova N., 2008, ApJS, 174, 223
Byckling K., Mukai K., Thorstensen J. R., Osborne J. P., 2010, MNRAS, 408, 2298
Cohn H. N. et al., 2010, ApJ, 722, 20
Cool A. M., Grindlay J. E., Bailyn C. D., Callanan P. J., Hertz P., 1995, ApJ, 438, 719
Curtin C., Shafter A. W., Pritchet C. J., Neill J. D., Kundu A., Maccarone T. J., 2015, ApJ, 811, 34
Dieball A., Long K. S., Knigge C., Thomson G. S., Zurek D. R., 2010, ApJ, 710, 332
Dobrotka A., Lasota J.-P., Menou K., 2006, ApJ, 640, 288
Edmonds P. D., Gilliland R. L., Heinke C. O., Grindlay J. E., 2003a, ApJ, 596, 1177
Edmonds P. D., Gilliland R. L., Heinke C. O., Grindlay J. E., 2003b, ApJ, 596, 1197
Eggleton P. P., 1983, ApJ, 268, 368
Eze R. N. C., 2015, Mem. Soc. Astron. Ital., 86, 96
Ferrario L., de Martino D., Gänsicke B. T., 2015, Space Sci. Rev., 191, 111
Fregeau J. M., Cheung P., Portegies Zwart S. F., Rasio F. A., 2004, MNRAS, 352, 1
Fukushige T., Heggie D. C., 2000, MNRAS, 318, 753
Gänsicke B. T. et al., 2009, MNRAS, 397, 2170
Geller A. M., Leigh N. W. C., 2015, ApJ, 808, L25
Giersz M., 1998, MNRAS, 298, 1239
Giersz M., 2001, MNRAS, 324, 218
Giersz M., 2006, MNRAS, 371, 484
Giersz M., Heggie D. C., Hurley J. R., 2008, MNRAS, 388, 429
Giersz M., Heggie D. C., Hurley J. R., Hypki A., 2013, MNRAS, 431, 2184
Giersz M., Leigh N., Hypki A., Lützgendorf N., Askar A., 2015, MNRAS, 454, 3150
Grindlay J. E., 2006, Adv. Space Res., 38, 2923
Grindlay J. E., Cool A. M., Callanan P. J., Bailyn C. D., Cohn H. N., Lugger P. M., 1995, ApJ, 455, L47
Hameury J.-M., Menou K., Dubus G., Lasota J.-P., Hure J.-M., 1998, MNRAS, 298, 1048
Harrop-Allin M. K., Warner B., 1996, MNRAS, 279, 219
Heinke C. O., Ruiter A. J., Muno M. P., Belczynski K., 2008, in Bandyopadhyay R. M., Wachter S., Gelino D., Gelino C. R., eds, AIP Conf. Ser. Vol. 1010, A Population Explosion: The Nature and Evolution of X-ray Binaries in Diverse Environments. Am. Inst. Phys., New York, p. 136
Hellier C., 2001, Cataclysmic Variable Stars. Springer, New York
Hénon M. H., 1971, Ap&SS, 14, 151
Hobbs G., Lorimer D. R., Lyne A. G., Kramer M., 2005, MNRAS, 360, 974
Howell S. B., Rappaport S., Politano M., 1997, MNRAS, 287, 929
Huang R. H. H., Becker W., Edmonds P. D., Elsner R. F., Heinke C. O., Hsieh B. C., 2010, A&A, 513, A16
Hurley J. R., Pols O. R., Tout C. A., 2000, MNRAS, 315, 543
Hurley J. R., Tout C. A., Pols O. R., 2002, MNRAS, 329, 897
Hypki A., Giersz M., 2013, MNRAS, 429, 1221
Hypki A., Giersz M., 2016a, preprint (arXiv:1604.07033)
Hypki A., Giersz M., 2016b, preprint (arXiv:1604.07054)
Iben I., Jr, Livio M., 1993, PASP, 105, 1373

Ivanova N., Heinke C. O., Rasio F. A., Taam R. E., Belczynski K., Fregeau J., 2006, MNRAS, 372, 1043
Knigge C., 2012, Mem. Soc. Astron. Ital., 83, 549
Knigge C., Zurek D. R., Shara M. M., Long K. S., Gilliland R. L., 2003, ApJ, 599, 1320
Knigge C., Baraffe I., Patterson J., 2011, ApJS, 194, 28
Kroupa P., 1995, MNRAS, 277, 1491
Kroupa P., 2001, MNRAS, 322, 231
Kroupa P., 2008, in Aarseth S. J., Tout C. A., Mardling R. A., eds, Lecture Notes in Physics, Vol. 760, The Cambridge N-Body Lectures. Springer, Berlin, p. 181
Kroupa P., 2011, in Alves J., Elmegreen B. G., Girart J. M., Trimble V., eds, Proc. IAU Symp. 270, Computational Star Formation. Cambridge Univ. Press, Cambridge, p. 141
Kroupa P., Gilmore G., Tout C. A., 1991, MNRAS, 251, 293
Kroupa P., Tout C. A., Gilmore G., 1993, MNRAS, 262, 545
Kroupa P., Weidner C., Pflamm-Altenburg J., Thies I., Dabringhausen J., Marks M., Maschberger T., 2013, in Oswalt T. D., Gilmore G., eds, Planets, Stars and Stellar Systems, Vol. 5. Springer, Berlin, p. 115
Lada C. J., Lada E. A., 2003, ARA&A, 41, 57
Lasota J.-P., 2001, New Astron. Rev., 45, 449
Leigh N. W. C., Giersz M., Marks M., Webb J. J., Hypki A., Heinke C. O., Kroupa P., Sills A., 2015, MNRAS, 446, 226
Leigh N. W. C., Geller A. M., Toonen S., 2016, ApJ, 818, 21
Littlefair S. P., Dhillon V. S., Marsh T. R., Gänsicke B. T., Southworth J., Watson C. A., 2006, Science, 314, 1578
Marks M., Kroupa P., 2012, A&A, 543, A8
Marks M., Kroupa P., Oh S., 2011, MNRAS, 417, 1684
Mukai K. et al., 2014, preprint (arXiv:1412.1163)
Olech A., Rutkowski A., Schwarzenberg-Czerny A., 2007, Acta Astron., 57, 331
Paczyński B., 1967, Acta Astron., 17, 287
Paczynski B., 1976, in Eggleton P., Mitton S., Whelan J., eds, Proc. IAU Symp. 73, Structure and Evolution of Close Binary Systems. Reidel, Dordrecht, p. 75
Paczynski B., Schwarzenberg-Czerny A., 1980, Acta Astron., 30, 127
Patterson J., 2011, MNRAS, 411, 2695
Patterson J., Raymond J. C., 1985, ApJ, 292, 535
Pietrukowicz P., 2009, Acta Astron., 59, 291
Pietrukowicz P., Kaluzny J., Schwarzenberg-Czerny A., Thompson I. B., Pych W., Krzeminski W., Mazur B., 2008, MNRAS, 388, 1111
Pooley D., 2010, Proc. Natl. Acad. Sci., 107, 7164
Pretorius M. L., Knigge C., Kolb U., 2007, MNRAS, 374, 1495
Rappaport S., Joss P. C., Webbink R. F., 1982, ApJ, 254, 616
Rappaport S., Verbunt F., Joss P. C., 1983, ApJ, 275, 713
Servillat M., Webb N. A., Lewis F., Knigge C., van den Berg M., Dieball A., Grindlay J., 2011, ApJ, 733, 106
Shakura N. I., Sunyaev R. A., 1973, A&A, 24, 337
Shara M. M., Bergeron L. E., Gilliland R. L., Saha A., Petro L., 1996, ApJ, 471, 804
Shara M. M., Zurek D. R., Baltz E. A., Lauer T. R., Silk J., 2004, ApJ, 605, L117
Shara M. M., Hinkley S., Zurek D. R., 2005, ApJ, 634, 1272
Smak J., 1996, Acta Astron., 46, 377
Smak J., 1999, Acta Astron., 49, 391
Smak J., 2001, in Lázaro F. C., Arévalo M. J., eds, Lecture Notes in Physics, Vol. 563, Binary Stars: Selected Topics on Observations and Physical Processes. Springer-Verlag, Berlin, p. 110
Spitzer L., 1987, Dynamical Evolution of Globular Clusters. Princeton Univ. Press, Princeton, NJ
Stodółkiewicz J. S., 1986, Acta Astron., 36, 19
Thomson G. S. et al., 2012, MNRAS, 423, 2901
Torres G., 2010, AJ, 140, 1158
Wang L. et al., 2016, MNRAS, 458, 1450
Warner B., 1995, Cambridge Astrophysics Series Vol. 28, Cataclysmic Variable Stars. Cambridge Univ. Press, Cambridge
Webb N. A., Servillat M., 2013, A&A, 551, A60
Webbink R. F., 1984, ApJ, 277, 355
Wickramasinghe D. T., Ferrario L., 2000, PASP, 112, 873
Zorotovic M. et al., 2016, MNRAS, 457, 3867

APPENDIX A: ABBREVIATIONS

In this appendix, we define all the abbreviations used in this work in order to provide the reader with an easy way to recognize them instead of going back through the text.

BD	brown dwarf
BSE	binary stellar evolution
CEP	common envelope phase
CV	cataclysmic variable
DIM	disc instability model
DNe	dwarf novae
GC	globular cluster
IBP	initial binary population
IMF	initial mass function
MS	main sequence
PDP	present-day population
SDI	strong dynamical interaction
WD	white dwarf
WDI	weak dynamical interaction

This paper has been typeset from a TEX/LATEX file prepared by the author.